University College of Southeast Norway

www.usn.no

FMH606 Master's Thesis 2017

Process Technology

Waste heat availability in the raw meal department of a cement plant

Widuramina Sameendranath Amarasinghe

University College of Southeast Norway

www.usn.no

Course: FMH606 Master's Thesis, 2017

Title: Waste heat availability in the raw meal department of a cement plant

Number of pages: 85

Keywords: Cement, Drying, Heat exchanger, Heat recovery, Waste heat

Student:	Widuramina Sameendranath Amarasinghe
Supervisor:	Professor Lars-Andre Tokheim
External partner:	Norcem As Brevik (Mrs. Ida Husum, Manager of Process and Environment)
Availability:	Open

Approved for archiving: _____

(supervisor signature)

Summary:

The main aim of this study was to find out the available heat of the exhaust gas stream that is bypassed through the raw meal department at Norcem Brevik cement plant, Norway which produces about 1 million ton of clinker per year. The study has been conducted for different process conditions in order to recover the available heat.

Mass and energy balance was performed for the raw meal department with the use of plant process database and manual measurements to calculate the available heat. Available heat is presented in two different end temperatures, 130 °C for LP steam generation and 50 °C for hot water generations. Sankey diagrams have been used to illustrate the available heat graphically.

It has been found that waste heat varies in between 4.2 MW to 1.5 MW for LP steam generation and 2.2 MW to 5.8 MW for hot water generation at the bypass line. The available heat is low when STD type is running compared to other process conditions. Approximately a heat of 20 MW for LP steam generation and 6 MW for hot water generation is available at the conditioning tower before the raw meal department when AFM is not running.

A network of heat exchangers is suggested to recover heat. The heat loss from the system and power inputs from fans and motors is negligible compared to the available heat.

It has been found that there is no gas recycling via the bypass line. Furthermore, the total false air coming into the system from different locations has been estimated as 40-50% of total air going out from the raw meal department. In addition, the behavior of moisture content, oxygen content and dust content of the gas streams have been discussed.

Preface

This thesis work is presented in partial fulfillment of the Master of Science degree in Process Technology at University College of South-east Norway (HSN). This work was performed at HSN and Norcem As Brevik under the supervision of Professor. Lars Andre Tokheim and Mrs. Ida Husum.

First, I would like to give my heartful gratitude to my main supervisor Professor. Lars Andre Tokheim for guiding me throughout this study with his great knowledge in a more schematic manner while having a good freedom and flexibility with the topics and discussions. And I would also like to thank my thesis co-supervisor Mrs. Ida Husum for guiding me with required information and encouraging me to fulfill the task by spending her valuable time.

I also would like to convey my gratitude to Mr. Thomas Thomassen, Mr. Jorn Tore Haglund, Mr. Per Gunnar Bund, Mr. Arnstein Jakobsen, Mr. Kjell Magnus Nilsen, Mr. Ketil Svinning at Norcem who gave guidance to me and shared their knowledge with me.

I would like to thank Mr. Amila Chandra at HSN, Mr. Jøran Sandberg and Mr. Sindre Strom at Norcem for the assistance given to me during velocity measurements at gas lines.

I must specially thank my beloved wife Anupama Wathsalani who was with me all the time and for giving great support. Finally, I would like to thank my parents who supported me throughout my entire education endeavor.

I hope you enjoy your reading!

Porsgrunn, May 1st, 2017

Widuramina Sameendranath Amarasinghe

Nomenclature

Abbreviations

Symbol	Description
A	Atmospheric air
AFM	Aero-fall mill
BF	Bag filter
BP	Bypass
CS	Coarse separator
CT	Conditioning tower
ESP	Electro-static precipitator
F	Gas cleaning equipment (Electro-static precipitator and Bag filter)
FF	Filter fan
FSA	Fullscreen analyzer
G	Gas
GS	Gas separation point
HGF	Hot gas fan
HS	High strength raw meal (Type HS)
LP	Low-pressure (steam)
M	AFM motor
MF	Main fan
RM	Raw material
STD	Standard raw meal (STD type)
Yr	Year

Roman Symbols

Symbol	Description	Units
A_s	Surface area of the particle	$[m^2]$
A_{sur}	Surface area of the pipelines and equipment	$[m^2]$
Bi	Biot number	$[-]$
$C_{Dust,in}$	Concentration of dust in the inlet gas stream coming into the raw meal department	$[g/Nm^3]$
$Cp_A(T)$	Specific heat capacity of the atmospheric air[1]	$[J/(kg.K)]$
$Cp_G(T)$	Specific heat capacity of the gas[1]	$[J/(kg.K)]$
$Cp_{RM}(T)$	Specific heat capacity of the raw materials[1]	$[J/(kg.K)]$
C_t	Thermal capacitance	$[J/K]$
D	Diameters of the circular gas pipelines	$[m]$
D_p	Average particle diameter	$[m]$
$Dust_{AFM,\,in}$	Mass flow rate of dust in the gas stream which is sent to the aero-fall mill (AFM)	$[kg/s]$
$Dust_{\,AFM,\,out}$	Mass flow rate of dust of the gas stream that coming out from the cyclone system	$[kg/s]$
$Dust_{\,BP}$	Mass flow rate of dust of the gas stream that going with the bypass gas stream	$[kg/s]$
$Dust_{ESP3,\ \ out}$	Dust mass flow rate coming out from the ESP (no.3) along with the hot gas stream	$[kg/s]$
$Dust_{\,F,\,in}$	Mass flow rate of dust of the gas stream which is sent to the electrostatic precipitator (ESP) and Bag filter (BF)	$[kg/s]$
$Dust_{\,in}$	Mass flow rate of dust in the inlet gas stream coming into the raw meal department	$[kg/s]$
$Dust_{out}$	Mass flow rate of dust of the gas stream which is going out from the raw meal department	$[kg/s]$

[1] here T indicates that parameter is a function of temperature. E.g. $h_s(T)$ indicates that h_s depends on temperature

$Dust_{tower,\ out}$	Dust mass flow rate coming out from the cyclone tower number 2 (preheating tower) along with the hot gas stream	$[kg/s]$
$h_s(T)$	Total specific enthalpy of steam	$[kJ/kg]$
k	Limestone thermal conductivity (Average value)	$[W/(m.K)]$
L	Latent heat of evaporation of water	$[J/kg]$
L_c	Characteristic length of particles	$[m]$
M_{wA}	Molecular weight of atmospheric air	$[kg/mol]$
M_{wG}	Molecular weight of gas	$[kg/mol]$
M_{wH_2O}	Molecular weight of moisture (water)	$[kg/mol]$
$\dot{m}_{A,\ AFM\ in}$	Mass flow rate of the false atmospheric air stream coming into the AFM via the raw material entrance opening	$[kg/s]$
$\dot{m}_{A,\ F\ in}$	Mass flow rate of the false atmospheric air stream coming into the BF and ESP	$[kg/s]$
$\dot{m}_{BF,\ out}$	Mass flow rate of raw meal powder that coming out from the BF	$[kg/s]$
$\dot{m}_{CS,\ out}$	Total mass flow rate of the crushed raw meal powder that coming out from the coarse separator	$[kg/s]$
$\dot{m}_{CT,in}$	Average mass flow rate of the gas stream before the conditioning tower	$[kg/s]$
$\dot{m}_{Cyclone,\ out}$	Total mass flow rate of the crushed raw meal powder that coming out from the cyclone system	$[kg/s]$
$\dot{m}_{G,\ AFM\ in}$	Mass flow rate of the gas stream which is sent to the AFM	$[kg/s]$
$\dot{m}_{G,\ AFM\ out}$	Mass flow rate of the gas stream coming out from AFM, coarse separator, and the cyclone system	$[kg/s]$
$\dot{m}_{G,\ BP}$	Mass flow rate of the gas stream which is bypassed the raw meal department	$[kg/s]$
$\dot{m}_{G,F,in}$	Mass flow rate of the mixed gas stream which is sent to the ESP and BF (bypass gas stream + gas stream coming from the raw meal department)	$[kg/s]$
$\dot{m}_{G,\ in}$	Mass flow rate of the gas stream coming into the raw meal department	$[kg/s]$
$\dot{m}_{G,\ out}$	Mass flow rate of the gas stream which is coming out from the ESP and BF and released to the atmosphere	$[kg/s]$

$\dot{m}_{H_2O}$	Mass flow rate of hot water generated	$[kg/s]$
$\dot{m}_{H_2O,CT}$	Water mass flow rate which is added to the gas stream at the conditioning tower	$[kg/s]$
$\dot{m}_{H_2O,CT,in}$	Water/moisture mass flow rate in the gas stream that coming into the conditioning tower	$[kg/s]$
$\dot{m}_{H_2O,in}$	Water/moisture mass flow rate of the gas stream which is coming into the raw meal department	$[kg/s]$
$\dot{m}_{RM,\ in}$	Total raw material mass flow rate coming into the AFM (limestone + additives) – Defined as moisture content inclusive	$[kg/s]$
$\dot{m}_{RM,\ tower,\ in}$	Raw meal into cyclone tower number 2 (preheating tower)	$[kg/s]$
$\dot{m}_{steam}$	Mass flow rate of LP steam generated	$[kg/s]$
$n_{flow\ rate}$	Mole flow rate of gas	$[mol/s]$
P	Pressure in the control volume	$[Pa]$
P_{BP}	Gauge pressure inside the bypass gas stream	$[mbar]$
P_{FF}	Power input from the filter fan	$[kW]$
P_{HGF}	Power input from the hot gas fan	$[kW]$
P_{in}	Downstream gas pressure of a fan	$[Pa]$
P_M	Motor power input to the AFM	$[MW]$
P_{MF}	Power input from the main fan	$[kW]$
P_N	Normal gas pressure	$[Pa]$
P_{out}	Upstream gas pressure of a fan	$[Pa]$
Q	Available heat	$[MW]$
$Q_{AFM,in}$	Heat load sent to the AFM (reference to 0 °C)	$[MW]$
$Q_{gain,\ AFM}$	Total heat gain by the raw materials, moisture, false air including the heat losses at AFM	$[MW]$
Q_{HW}	Available heat for hot water generation	$[MW]$
$Q_{HW,\ CT}$	Available heat for hot water generation at the conditioning tower when AFM is not running	$[TJ/yr]$

$Q_{in,\ GS}$	Energy entering to the gas separating point	$[MW]$
$Q_{input,\ AFM}$	Total heat released from the hot gas stream at the AFM and the power input from the AFM motor (P_M)	$[MW]$
Q_{LP}	Available heat for LP steam generation	$[MW]$
$Q_{LP,\ CT}$	Available heat for LP steam at the conditioning tower when AFM is not running	$[TJ/yr]$
Q_{loss}	Heat loss	[W]
$Q_{out,\ GS}$	Energy going out from the gas separating point	$[MW]$
$T_{A,\ in}$	Atmospheric air temperature	$[°C]$
T_{CT}	Average gas temperature before the conditioning tower	$[°C]$
T_f	Final temperature of Particles	$[°C]$
$T_{Fan,in}$	Gas inlet temperature for the fan	$[K]$
$T_{G,\ AFM\ in}$	Temperature of the gas stream which is sent to the AFM	$[°C]$
$T_{G,\ AFM\ out}$	Temperature of the gas stream coming out from AFM, coarse separator, and the cyclone system	$[°C]$
$T_{G,\ BP}$	Temperature of the gas stream which is bypassed the raw meal department	$[°C]$
$T_{G,F,in}$	Temperature of the mixed gas stream which is sent to the ESP and BF (bypass gas stream + gas stream coming from the raw meal department)	$[°C]$
$T_{G,\ in}$	Gas temperature which is coming from the preheater tower	$[°C]$
$T_{G,\ out}$	Temperature of the gas stream which is coming out from the ESP and BF and released to the atmosphere	$[°C]$
$T_{HW,\ in}$	Inlet temperature of the water used to generate hot water	$[°C]$
$T_{HW,\ out}$	Temperature of the hot water generated	$[°C]$
T_i	Initial temperature of Particles	$[°C]$
T_N	Normal temperature	$[K]$
T_{ref1}	End temperature 1 (130 °C)	$[°C]$
T_{ref2}	End temperature 2 (50 °C)	$[°C]$

$T_{RM,\ in}$	Raw material temperature which is coming into the raw meal department	$[°C]$
$T_{RM,\ out}$	Temperature of the raw material stream which is coming out from the coarse separator and the cyclone system	$[°C]$
T_{sur}	Surface temperature of the pipelines and the equipment	$[°C]$
T_{∞}	Average gas temperature inside the coarse separator and cyclones	$[°C]$
$t_{AFM\ downtime}$	Assumed downtime of the AFM per week	$[h/week]$
t_f	Residence time of the particles	$[s]$
U	Average overall heat transfer coefficient from surfaces to air	$[W/(m^2.K)]$
V	Volume of a particle	$[m^3]$
$\dot{V}_{A,\ AFM\ in}$	Volumetric flow rate of the false atmospheric air stream coming into the AFM via the raw material entrance opening	$[Nm^3/s]$
$\dot{V}_{A,\ F\ in}$	Volumetric flow rate of the false atmospheric air stream coming into the ESP and BF	$[Nm^3/s]$
$\dot{V}_{CT,in}$	Volumetric flow rate of the gas stream before the conditioning tower	$[Nm^3/s]$
$\dot{V}_{G,\ AFM\ in}$	Volumetric flow rate of the gas stream which is sent to the AFM	$[Nm^3/s]$
$\dot{V}_{G,\ AFM\ out}$	Volumetric flow rate of the gas stream coming out from AFM, coarse separator, and the cyclone system	$[Nm^3/s]$
$\dot{V}_{G,\ BP}$	Volumetric flow rate of the gas stream which is bypassed the raw meal department	$[Nm^3/s]$
$\dot{V}_{G,F,in}$	Volumetric flow rate of the mixed gas stream which is sent to the ESP and BF (bypass gas stream + gas stream coming from the raw meal department)	$[Nm^3/s]$
$\dot{V}_{G,\ in}$	Volumetric flow rate of the gas stream coming into the raw meal department	$[Nm^3/s]$
$\dot{V}_{G,\ out}$	Volumetric flow rate of the gas stream which is coming out from the ESP and BF and released to the atmosphere	$[Nm^3/s]$
$v_{G,\ AFM\ in}$	Average velocity of the gas stream which is sent through to the AFM	$[m/s]$

$v_{G,\ BP}$	Average velocity of the gas stream which is bypassed the raw meal department	$[m/s]$
$v_{G,\ in}$	Average velocity of the gas stream coming from the preheater tower	$[m/s]$
W_{el}	Fan power (electricity)	$[W]$
$Weeks_{kiln}$	No of kiln running weeks in a year	$[weeks/yr]$
$x_{H_2O,\,RM,\ in}$	Total moisture mass fraction of all the raw materials coming into the AFM (limestone + additives)	$[-]$
$x_{H_2O,\,RM,\ out}$	Total moisture mass fraction of the all crushed raw meal powder that coming out from the coarse separator and the cyclone system	$[-]$
$X_{\,Dust}$	The ratio of the heat carrying capacity by the dust stream inside the bypass line to the heat carrying capacity by the total gas stream inside the bypass line	$[-]$
$y_{H_2O,\,A,\ in}$	Moisture volume fraction of the atmospheric air	$[-]$
$y_{H_2O,\ AFM\ in}$	Moisture volume fraction of the gas stream which is sent to the AFM	$[-]$
$y_{H_2O,\,BP}$	Moisture volume fraction of the gas stream which is bypassed the raw meal department	$[-]$
$y_{H_2O,CT,in}$	Moisture volume fraction in the gas stream that coming into the conditioning tower	$[-]$
$y_{H_2O,\,G,\,AFM\ out}$	Moisture volume fraction of the gas stream coming out from AFM, coarse separator, and the cyclone system	$[-]$
$y_{H_2O,\,G,\,F,\,in}$	Moisture volume fraction of the mixed gas stream which is sent to the ESP and BF (bypass gas stream + gas stream coming from the raw meal department)	$[-]$
$y_{H_2O,G,\,in}$	Moisture volume fraction of the gas stream coming from the preheater tower	$[-]$
$y_{H_2O,\,G,\,out}$	Moisture volume fraction of the gas stream which is coming out from the ESP and BF and released to the atmosphere	$[-]$
$y_{O_2,\,A,\,in}$	Atmospheric oxygen volume fraction	$[-]$
$y_{O_2,\ AFM\ in}$	Oxygen volume fraction of the gas stream which is sent to the AFM	$[-]$
$y_{O_2,\ BP}$	Oxygen volume fraction of the gas stream which is bypassed the raw meal department`	$[-]$

$y_{O_2,\ G,\ AFM\ out}$	Oxygen volume fraction of the gas stream coming out from AFM, coarse separator, and the cyclone system	$[-]$
$y_{O_2,\ G,\ F,\ in}$	Oxygen volume fraction of the mixed gas stream which is sent to the ESP and BF (bypass gas stream + gas stream coming from the raw meal department)	$[-]$
$y_{O_2,G,\ in}$	Oxygen volume fraction of the gas stream coming from the preheater tower	$[-]$
$y_{O_2,\ G,\ out}$	Oxygen volume fraction of the mixed gas stream which is coming out from the ESP and BF and released to the atmosphere	$[-]$

Greek Letters

Symbol	Description	Units
η_{BF}	Bag filter efficiency	$[-]$
η_{CS}	Coarse separator efficiency	$[-]$
$\eta_{Cyclone}$	Cyclone tower/system efficiency	$[-]$
η_{ESP}	Electro-static precipitator efficiency	$[-]$
η_{fan}	Fan efficiency	$[-]$
ρ_{H_2O}	Density of the moisture in gas (At normal conditions)	$[kg/Nm^3]$
ρ_A	Density of the atmospheric air (At normal conditions)	$[kg/Nm^3]$
ρ_G	Density of the gas (At normal conditions)	$[kg/Nm^3]$
ρ_{RM}	Density of Limestone	$[kg/m^3]$
τ	Thermal time constant	$[s]$

Physical Constants

Constant	Value	Units
Cp_{H_2O} - Specific heat capacity of water	4185	$[J/kg.K]$
M_{wH_2O}- Molecular weight of water	0.018	$[kg/mol]$
P_N - Normal gas pressure	101325	$[Pa]$
T_N - Normal temperature	273.15	$[K]$
R - Universal gas constant	8.314	$[J/mol.K]$

Contents

List of Figures

List of Tables

1 Introduction

This chapter gives a small description about the Norcem-Brevik cement plant, a small description about the raw meal department, the importance of heat utilization of exhaust gas stream at the raw meal department and the problem description. Furthermore, the objectives of this study have been pointed out along with the key questions that should arise and the tasks that need to do to overcome them.

1.1 Background

The cement industry is one of main process industry in the world which has high energy intensive operations. Clinker production in the kiln is the main unit operation where more than 75% total energy of the plant is consumed. The exhaust gas coming out from the kiln is at high temperature and it carries higher sensible heat.

Norcem is the sole cement producer in Norway which has two major production facilities established in Brevik and Kjopsvik. Norcem produces and sells all types of cement for most of the industries in Norway. The Brevik production plant produces approximately 1 million tons of clinker per year [1]. Norcem Brevik uses three types of limestone to produce cement in order to produce different types of cement.

Norcem Brevik has a raw material processing department which is called “Raw meal Department” where limestone and additives are mixed, crushed and dried together to produce a mixture of fine powder of raw materials which is called as Raw meal. This raw meal is then sent to the cement kiln after preheating by the exhaust gas coming out from the kiln. Then the clinker coming out from the kiln is sent to cement mills for final cement production steps.

As exhaust gas coming out from the series of raw-meal preheaters, a part of the gas is sent through the raw meal department to dry the raw meal as well as to fulfill the purpose of pneumatic transportation of the raw meal powder. Other gas stream is bypassed the raw meal department. Then the gas stream which is sent via the raw meal department is mixed with the bypass gas stream after the raw meal department and sent via series of de-dusting operations and released to the atmosphere.

1.2 Problem description

The aim of this study is to figure out the waste heat availability in the bypass exhaust gas stream which bypasses the raw meal department. It has experienced that the bypassing gas does contain some sensible heat and can be utilized for other purposes such as generate low-pressure (LP) steam and hot water by installing a heat exchanger. Currently, this available extra heat is not utilized anywhere after the raw meal department and released to the atmosphere along with the gas stream.

Mainly Norcem Brevik produces two types of raw meals which are namely “standard raw meal” (STD) and “high strength raw meal” (HS) with different compositions of limestone types and other additives. So, the total drying heating requirement would be different for those two types of raw meal due to the variation in moisture content of limestone and additives that used to prepare the raw meal.

Depend on the which raw meal type is processed inside the raw meal department, the exhaust gas fraction bypasses the raw meal department changes due to the drying heating requirement and due to the gas flow rate requirement for the pneumatic transportation of powders. So, the

waste heat availability in the bypass gas stream would be different when the raw meal composition changes.

1.2.1 Objectives

The main objective of this master's thesis work is to quantify and compare the available waste heat under different operating conditions. In order to achieve the objective, the following tasks and questions are needed to be completed/answered.

1.2.2 Questions

- How much heat may be extracted from the hot gas during the production of two different raw meals (STD raw meal and HS raw meal) respectively?
- What is the variation in heat availability during normal operation conditions?
- What is the heat loss from raw mill system? Is it significant compared to the available heat?
- Is there any recycle (backflow) in the bypass gas stream? If so under what conditions that might occur?
- How much is false air coming into the raw meal department via aero-fall mill (AFM) and via electro-static precipitator (ESP) and bag filter (BF)?

1.2.3 Tasks

- Collect existing temperature, flow rate, composition, pressure data from Norcem Brevik
- Develop a mass and energy balance for the whole exhaust gas streams which is going through the raw meal department as well as the bypass stream while taking the raw material feed taking to account
- Run separate measurements if required for the mass and energy balance at Norcem Brevik
- Quantification and conclude about the waste heat availability in the raw meal department based on the calculations
- Find a relationship between waste heat availability vs valve opening of the flowing gas inside the raw meal department
- Make Suggestion to extract the available heat from the bypass gas stream

1.3 Thesis Outline

The thesis mainly contains 7 chapters. The first chapter gives an overall introduction to the topics along with background and problem description. In the problem description, the key objectives are pointed out by describing questions that need to be answered and the task that required to execute to get those answers. The first chapter also consists of a small literature review on heat recovery in cement plants.

The second chapter is mainly focusing on the process description. The key unit operations, material and gas flows are described extensively along with process flow diagrams and actual snaps of the process from Norcem Brevik. Chapter 3 describes the methods that were used to extract data, measure data and to illustrate the results. Model development is mainly described in chapter 4 along with necessary assumptions. Chapter 5 consists of necessary calculations required to generate the required final and intermediate results, and the calculations required to validate the assumptions made.

Chapter 6 is mainly describing the results of the overall calculations while discussing them. Furthermore, some key factors related to the process has been discussed while discussing the assumptions made during the model development. Chapter 7 gives an overall conclusion to the thesis along with suggestions and further work recommendations. There is an Appendices section followed by the references chapter which supports the proceedings of the main thesis. All the symbols used in the thesis are defined in the nomenclature.

1.4 Literature review

This small literature study has focused on how the waste heat utilization from the exhaust gas coming from the cement kiln is executed and possible heat extraction methods and key factors affect for the heat recovery.

In most of the cement plants, the exhaust gas flows from the kiln (via preheater system) contains useful sensible energy that released directly into the atmosphere. Generally, this gas temperature varies between 250 °C to 450 °C after the preheater towers (see subchapter 2.19 for a short description on preheater towers). Holcim cement group has a done study of waste heat recovery at norther Europe countries and according to the report, most of the northern European cement plant do have more than 20% of input heat for power generation [2].

Typically, modern cement plants use this hot gas flow coming from the preheater towers to dry raw material in the raw meal processing department [3]. The amount of available heat at the raw meal department can vary due to many reasons such as the moisture content of the raw feed, temperatures fluctuation due to the kiln operation etc. [4]. Furthermore, studies have found that the moisture content in the raw materials has an important influence on the sizing of the heat recovery system [5].

Another modern intensive to recover the exhaust gas heat and use for power generation. But most of the available studies are conducted to study the recoverability of the waste heat for power generation from the exhaust gas coming out from the preheater tower directly.

A typical system for recycling waste heat power generation includes heat exchangers or steam generators to transfer heat from exhaust gasses to heat carrying fluid. Turbines, electric generators, condensers and a cooling system for the working fluid are other main unit operation that consists in the power generation system [3]. Organic Rankine cycle (ORC) is a better system to recover waste heat to generate power by using water as the liquid fluid [2].

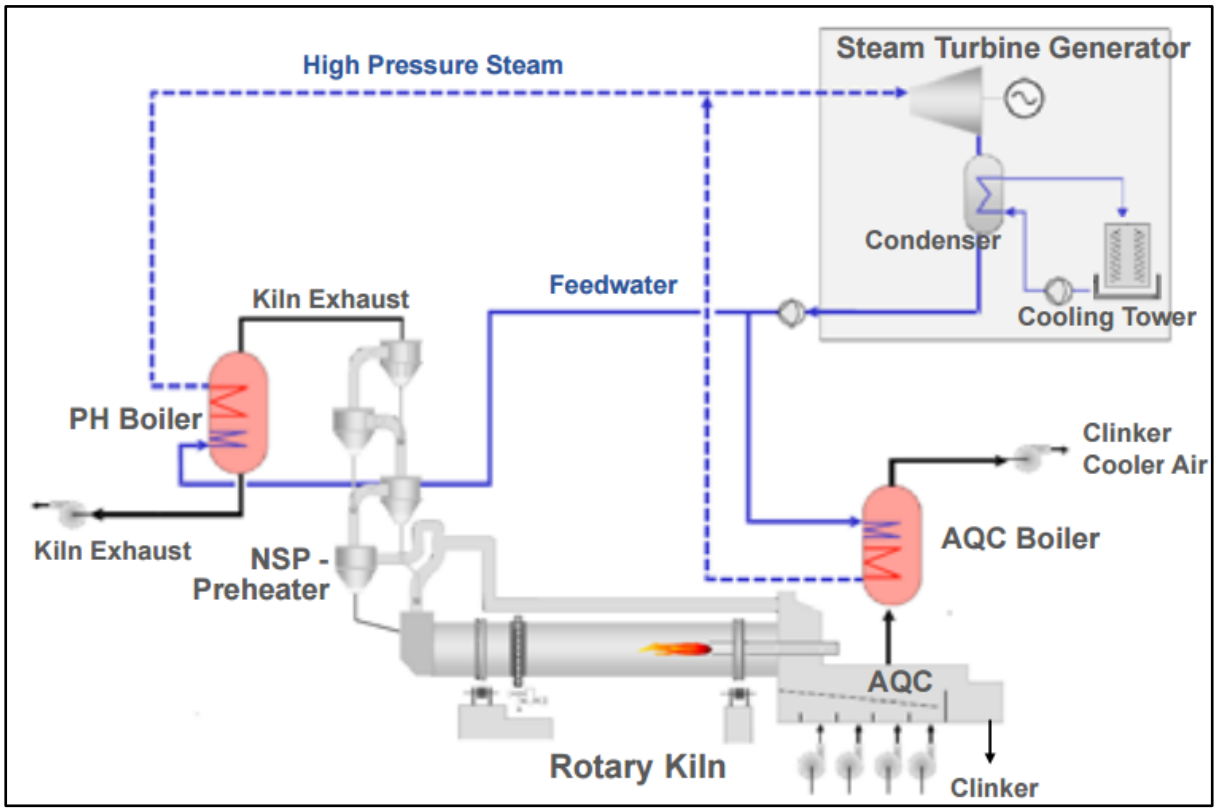

Figure 1-1: Waste heat recovery system to generate steam using the exhaust gas after the preheater towers [4]

Figure 1 1 shows a schematic diagram of a waste heat recovery system at Holcim Untervaz, Switzerland plant to generate steam using the exhaust gas after the preheater towers.

One of the key issues with the heat recovery from the exhaust gas coming from the preheater towers is accumulation of dust inside the heat exchangers. So, the heat exchanger design and the dust cleaning technology going to used is critical for a smooth process without any obstructions [2] [6].

2 Process Description

In this subchapter, the types of raw materials used for the cement production and main raw material recipes that are processed inside the raw material department are described. The individual unit operations/equipment in the raw meal department and the gas streams and raw material streams also have described briefly. The process flow diagram is shown in Figure 2-8 which has illustrated all the gas and material flows as well as all the unit operations/equipment in the raw meal department.

2.1 Raw materials

In Norcem Brevik, mainly three types of limestone are used for clinker production. One type of the limestone is excavated from the underground mine in Dalen at Brevik itself which goes more than 330 meters below sea level. Verdal mine is another quarry of limestone. The quality of Dalen and Verdal limestone types is very high (more than 95% pure). The other source of the limestone is at Bjorntvet as an open quarry which has a low quality compared to the Dalen and Verdal types.

Mainly Norcem Brevik produces two types of raw meals which are namely “standard raw meal” (STD type) and “high strength raw meal” (Type HS) with different compositions of limestone types and other additives. Limestone and additives are added to a belt which carries all the raw material as a single stream into the AFM to fulfill the crushing and drying purpose.

To produce STD type mixture of limestone from Dalen mine and Bjorntvet quarry is used. But to produce Type HS only the limestone from the Dalen mine and Verdal quarry is used which have higher purity as mentioned before.

Figure 2-1: Adding of additives into the raw material belt

Figure 2-2: Raw material mixture is going into the AFM

Currently Norcem Brevik uses Quartz, Slag, Copper ore (rich with iron ore) and Aluminum serox as main additives for the raw meal recipes. Adjust the quality of the final cement product

which is used for the different construction purposes is the main purpose of adding these additives to the limestone.

The raw material recipes for the main two cement types are shown in Table 2-1 while Figure 2-1 shows additives are added into the raw material conveying belt. Figure 2-2 shows the raw material mixture going into the AFM. At this raw material feeding point to the AFM, a significant amount of false air is sucked into the main gas streams.

Table 2-1: Raw material recipes for two main type of raw meal

Materials	**STD type - Mass Percentage (%)**	**Type HS - Mass Percentage (%)**
Limestone – High quality (From Dalen mine and Verdal mine)	45.51	83.92
Limestone - Low quality (From Bjorntvet quarry)	49.73	0
Quartz	3.71	9.82
Slag	0	0
Copper ore (rich with iron ore)	1.05	2.52
Aluminum serox	0	3.73

2.2 Raw material storage silos

There are raw material silos which supply limestone and additives to produce the required raw meal for the cement production. There are designated silos for all types of limestone. The additives are added accordingly from designated silos to produce required raw meal to achieve the final product quality.

Combined stream of limestone and additives are then sent to the AFM. A small amount of raw material stream (Raw material mixture already have some fraction of fine particles which have the required particle size) bypass the AFM and send to the roll press directly.

Before the raw material stream separate to two streams there is an online analyzing system established. The system is called Fullscreen analyzer, FSA (also identified as cross belt analyzer, CBA) which analyze the quality of raw materials at a higher frequency by checking the elemental composition of the materials using the principal of illuminating the material with neutrons [7]. The existing FSA at Norcem is unable to measure the moisture content of the materials.

2.3 Hot gas inlet stream

Hot gas coming into the raw meal department is the exhaust gas released from the main kiln. The temperature of the gas coming in vary depend on the type of raw material recipe which is processed in the kiln. Generally, hot gas temperature at the inlet to the raw meal department is approximately 180 °C for STD type and 260 °C for Type HS. The flow rate of this gas stream can be varying around 300 kNm^3/h during optimum production rate at the kiln. The gas stream composite with O_2, N_2, H_2O and CO_2 along with some other minor gasses such as SO_x and NO_x. There is a significant dust stream also coming along with this gas stream (Approximately 3 g/Nm^3) just because the gas stream is coming after it has gone through the preheater towers where the gas has a direct contact with the raw meal powder (see subchapter 2.19). The composition of the gasses in main inlet gas stream when HS raw meal type is in the process at kiln is shown in Table 2-2.

Table 2-2: Inlet gas stream composition when Type HS raw meal is in the process at kiln

Component	Value	Units
N_2	61.42	Vol %
CO_2	22.22	Vol %
O_2	7.03	Vol %
H_2O	5-12	Vol %
SO_2	0-500	$[ppm]$
Dust	3	$[g/Nm^3]$

2.4 Hot gas stream inside the raw meal department

Hot gas is separated into two streams as soon as it enters to the raw meal department. One stream is sent into the raw meal processing units while the other stream is bypassed. The bypassed stream is rejoined with the exit gas stream from the raw meal processing unit (gas stream coming out from the cyclone system). Figure 2-3 shows the point where the gas separates into two streams from the inlet hot gas stream.

2.5 Hot gas fan

Hot gas fan facilitates pressure gradient required for the inlet gas stream which coming out from the preheater tower to the raw meal department. The driving force, pressure gradient keep hot gas flow smooth. This draws approximately 180 kW during the optimum operating conditions. Figure 2-4 shows the location of the hot gas fan at the inlet hot gas stream pipe.

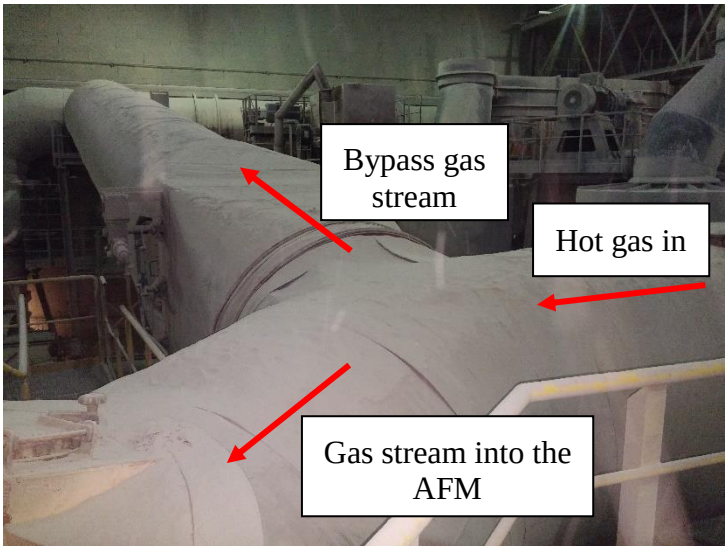

Figure 2-3: Gas separation point

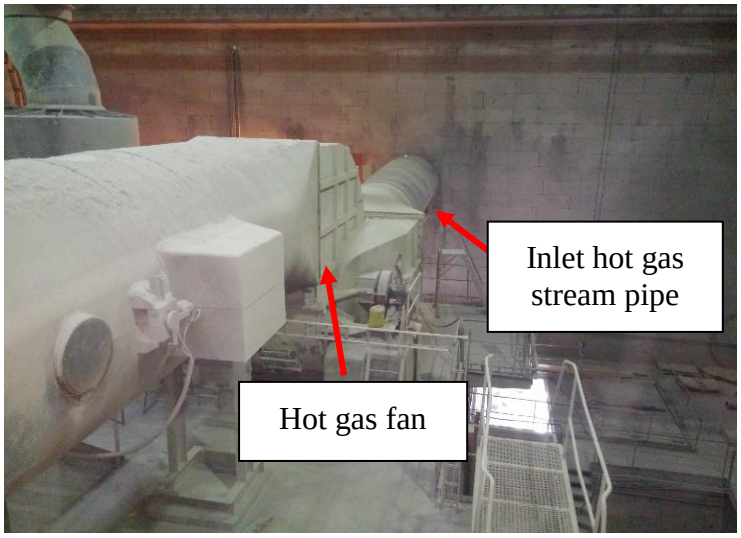

Figure 2-4: Hot gas fan location

2.6 Oil burner

The oil burner is established inside the raw meal department to dry the raw meal when there is no hot gas flow. i.e. when the kiln in not operating. Norcem always keeps a stock of dried raw meal inside storage silos to achieve a continuous process in the kiln. When the kiln is not operating, there is not hot gas available to continue the drying and crushing process inside the raw meal department. To overcome the heating requirement for the drying process this oil burner is used.

2.7 Air flow control valve

This is the valve which regulates the air flow fraction going through the AFM. Generally, the opening of this valve is around 60% when STD type raw meal recipe is processing while it varies around 40% when Type HS raw meal recipe is processing. The valve is located just before the main fan and just after the two cyclone units (see Figure 2-8 for the valve location).

2.8 Aero-fall mill (Ball mill)

The main purpose of the AFM is to grind the raw material for the first time. The AFM in Norcem Brevik raw meal department is about 10m diameter vertical mill with 2m width. The hot gas coming into the AFM has two purposes, to dry the raw meal mixture and transfer ground raw meal powder pneumatically to the coarse separator [8]. The flow rate of the hot gas is adjusted manually using air flow control valve such that the hot gas dries the raw meal completely as well as carry the ground raw meal out from the AFM. The average power consumption of the AFM is 1200 kW. Figure 2-5 shows the outside view of the actual AFM located at the raw meal department in Norcem Brevik and Figure 2-6 shows the inside view.

Figure 2-5: Outside view of the AFM

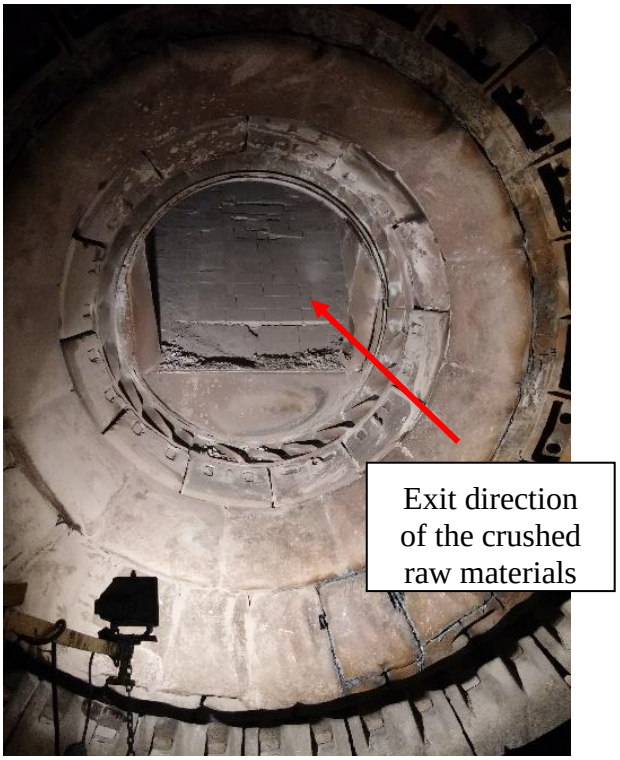

Figure 2-6: Inside view of the AFM

Figure 2-7: Coarse separator

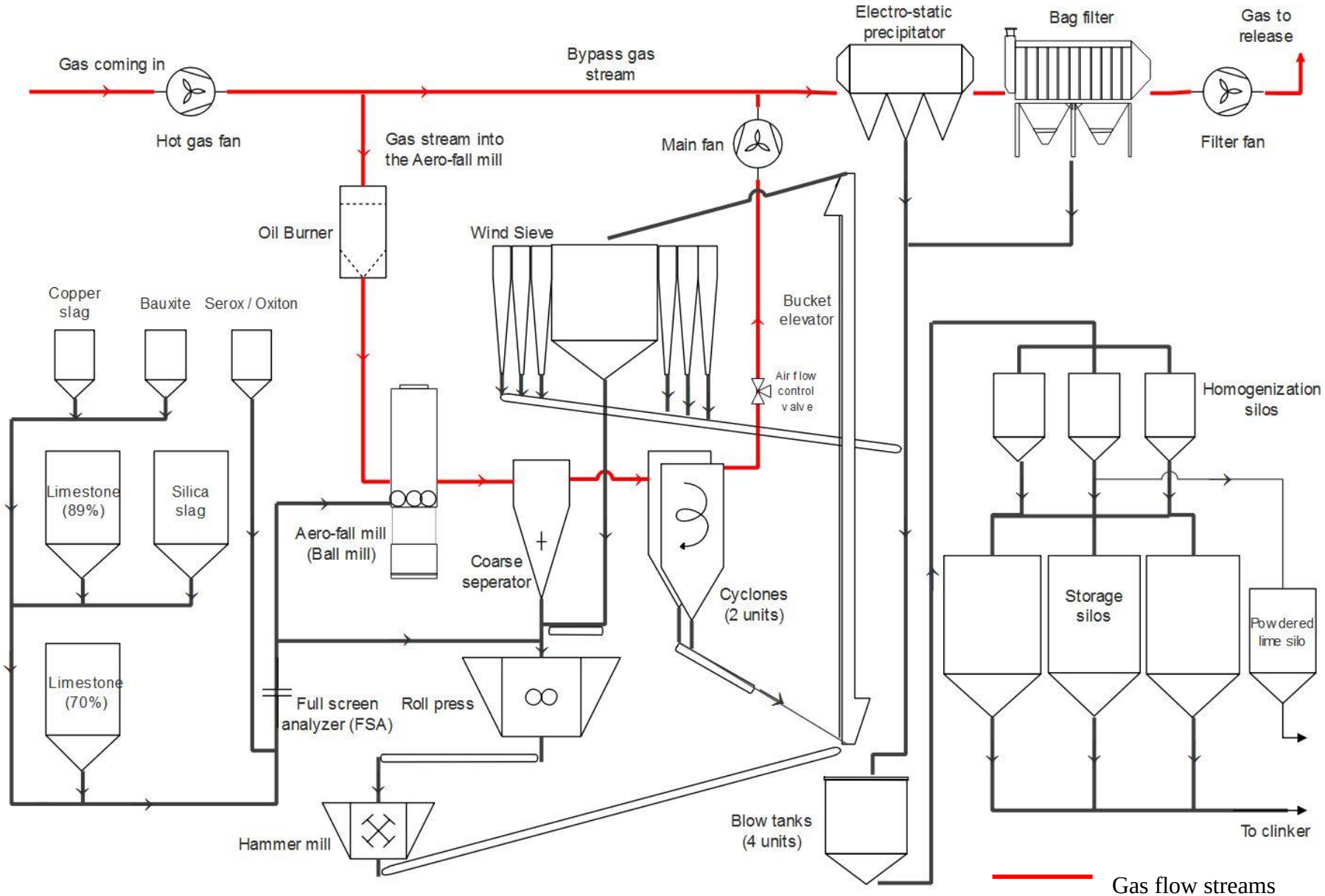

Figure 2-8: Process flow diagram of the raw meal department

2.9 Coarse separator

The gas stream which carries the ground and dried raw meal powder from AFM is sent via the coarse separator. This coarse separator simply acts as a gravity settler. It simply works using the principle of downward motion of particles under gravity when flowing horizontally [9]. The settled particles under gravity are collected (contain much larger particles) from the bottom of the separator and sent to the roller press. The gas stream (contain many fine particles) is sent to the cyclone system. But the efficiency of a coarse separator is low compared to other particle separation methods established in the raw meal department. Figure 2-7 shows an image of the coarse separator.

2.10 Cyclones

Gas flow is sent via a cyclone system followed by the coarse separator. There are two cyclones in presence where both act simultaneously in series. Typically, the efficiency of a cyclone is higher than a coarse separator. So, most of the raw meal powder is collected from the bottom of the cyclone. Even though cyclone collect most of the raw meal particles still the gas exiting the cyclone do contain finer raw meal powder. Figure 2-9 and Figure 2-10 shows the middle part and the bottom part of the two cyclones respectively.

Figure 2-9: Middle part of the two cyclones

Figure 2-10: Bottom part of the two cyclones

2.11 Roller press and hammer mill

The bottom collective of particles from the coarse separator is sent to a roller press for further grinding. Then ground raw meal powder is sent to a hammer mill via a transport belt to achieve more fine powder. At the bottom of Figure 2-8 it has shown the arrangement of the Roller press and hammer mill locations.

2.12 Bucket Elevator

The bottom streams from the cyclone system and hammer mill are combined and sent to a bucket elevator where fine raw meal powder is sent to air separator (Wind sieve).

2.13 Wind sieve

The Wind sieve separates fine powder from coarse particles using sieves. Here a recirculating compressed air stream is flowing to enhance the sieving process. The separated fine powder is sent to the blow tank system while coarse powder is sent back again to the roll press. A part of the wind sieve is shown in Figure 2-11.

2.14 Main fan

Figure 2-11: Part of the wind sieve

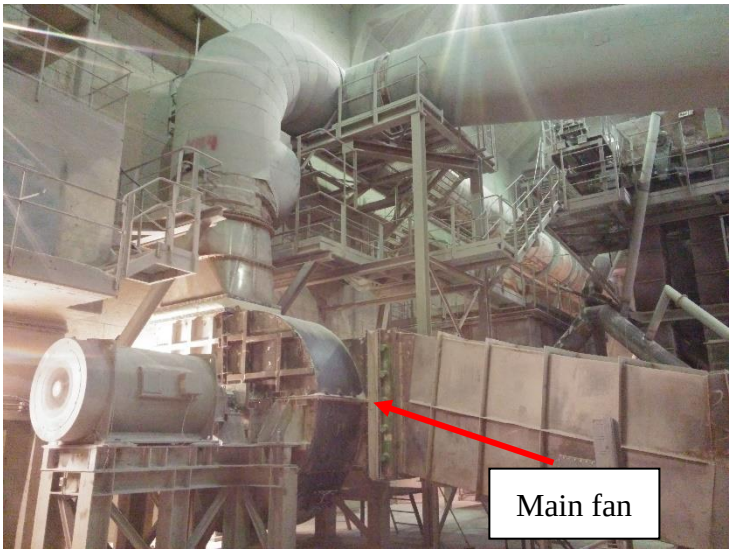

Figure 2-12: Main fan

The main fan provides required driving force for the hot gas to flow via the AFM, coarse separator, and the cyclone system by generating pressure gradient. Figure 2-12 shows the location of the main fan which is placed after the two cyclones system. After the main fan, the gas stream is joined back with the bypass gas stream and sent to the ESP and BF as shown in Figure 2-13. The main fan draws approximately 30 kW during the optimum operating conditions.

2.15 Electro-Static precipitator and Bag filter

As mentioned, the gas stream coming out from the cyclone system contain un-extracted fine powder. When that gas stream is combined with the bypassed gas stream the particle concentration gets diluted. But the particles need to be removed from the gas stream as much as possible before releasing to the atmosphere. To remove the particulate matter in the gas stream, a BF is used followed by an ESP. The removed particles are combined with the particle stream coming out of the Wind sieve (fine stream) and sent to the blow tank system (streams of particles can be seen in Figure 2-8). Since the particle removal efficiency is very higher in both ESP and BF for more fine particles, most of the particles in the gas stream in removed. From ESP and BF also a fraction of false air is sucked into the gas streams. ESP and the BF in Norcem Brevik are shown in Figure 2-14.

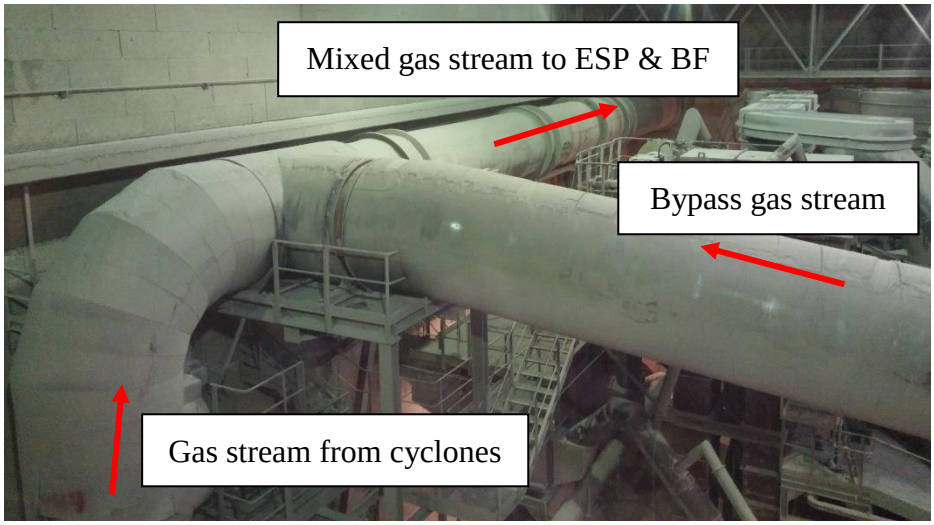

Figure 2-13: Gas streams mixing location

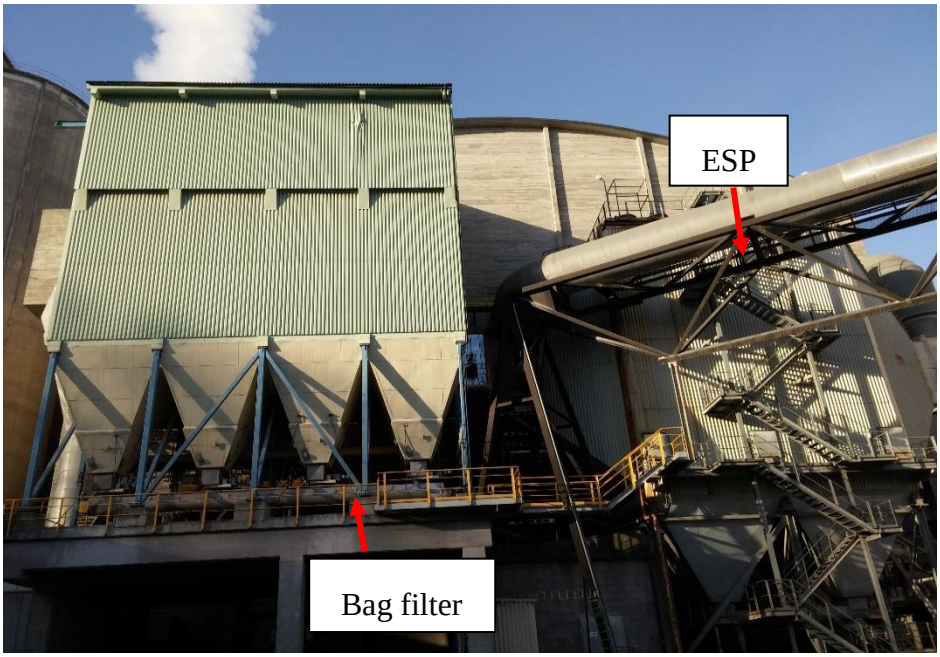

Figure 2-14: ESP and the Bag filter

2.16 Filter fan

Filter fan is used to add an extra driving force that is needed to the hot gas to flow via ESP and BF. Filter fan consumes approximately 300 kW during the optimum operating conditions.

2.17 Blow tank system

At Norcem Brevik raw meal department there are four blow tanks operating. Blow tank system is a good way to transfer powder in dense phase. They are operating separately to each other. For an example when one blow tank is pressurizing the particles fill another blow tank, another one`s pressure released etc.

2.18 Homogenization silos, Storage silos, and Powdered lime silo

After the blow tank, raw meal powder is sent to the holding silos and then filled to storage silos for later cement production requirement. A fraction of raw meal powder stream is taken separately and stored in a powdered lime silo for the current use.

2.19 Inlet gas stream path before the raw meal department

Figure 2-15 shows the path of the hot gas stream before entering to the raw meal department. The gas stream coming from the kiln is going through the preheater tower cyclone system to heat up the raw meal just before sending them to the pre-calciner. There are two cyclone towers. But only the gas stream going through one cyclone tower number 2 (see Figure 2-15) is sent to the raw meal department. The gas stream is passed via an ESP (no.3) followed by a conditioning tower before entering to the raw meal department. There are two fans, just before and after the ESP to add require driving force for the gas stream.

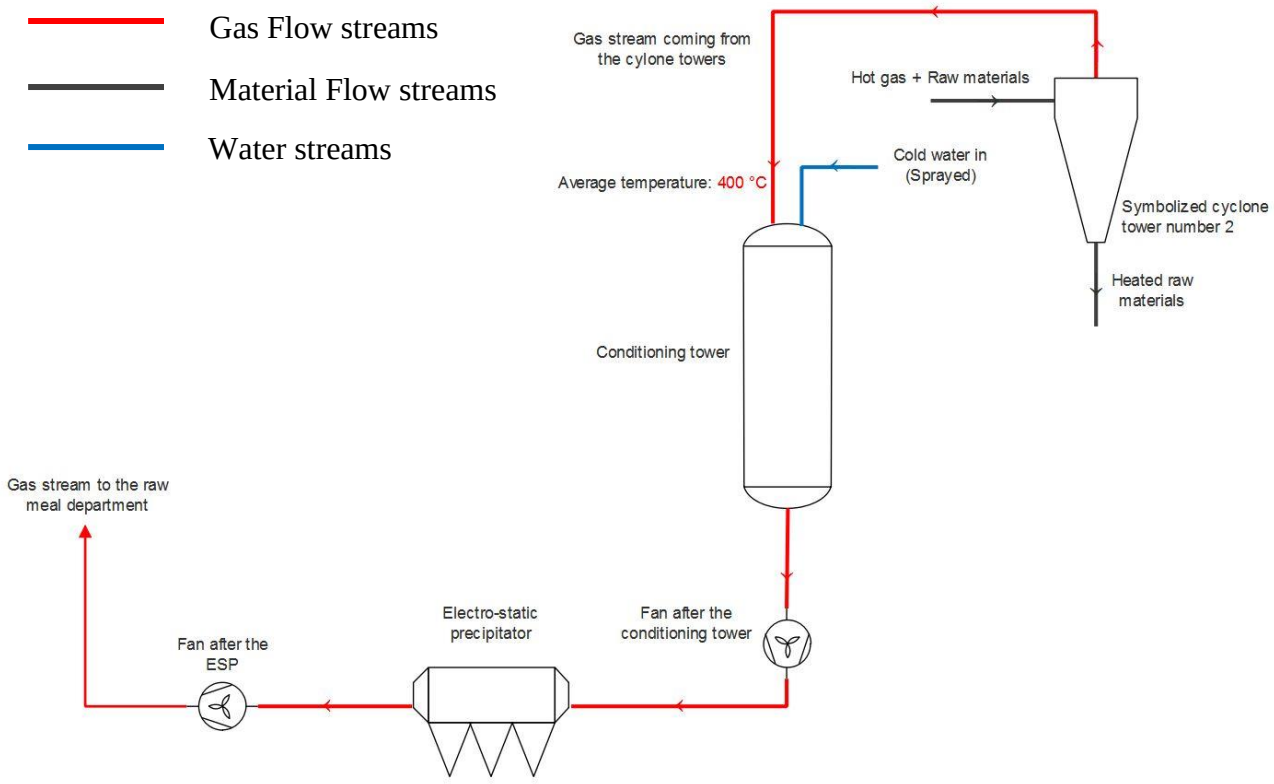

Figure 2-15: Inlet gas stream path before entering to the raw meal department

3 Method

3.1 Data acquisition

Boundary conditions, which depend on the raw meal type, were identified, and process data were utilized as inputs to the model. Continuous measurements logged in the plant process database were extracted, and additional manual measurements were carried out to close the model and to validate it.

3.2 Manual measurements

To measure the gas velocities at the inlet gas stream, bypass gas stream and before AFM, a pitot tube was used. Existing sample points openings were used to gain the access into the pipe.

To estimate the heat losses from critical points, the surface temperatures of the equipment, pipelines were measured using a laser thermometer. Several temperature measurements were taken near a location and an average surface temperature value was obtained.

3.3 Data Illustration

Energy streams and possible energy recovery streams are shown using Sankey diagrams. e!Sankey® trail version was used to draw the Sankey diagrams.

4 Model development

The model was established based on a mass and energy balance of the raw meal processing facility. Considered control volume of the system for the model development is shown in Figure 4-1 with numbered streams. In Figure 4-2 the block diagram for the considered volume is shown with all the parameters and units. Different color legends have been used to clearly identify the available values from the plant logged database, parameters that are available in literature and the variables that need to be calculated.

4.1 Assumptions

Several assumptions were made during the model development as shown below. Most of the assumptions made are discussed in the subchapter 6.4 to clarify further.

1. Heat capacity of raw material, exhaust gas, and atmospheric air are considered as temperature dependent
2. Atmospheric air moisture content and raw material moisture content that coming into the raw meal department is assumed constant at the considered moment
3. The individual moisture content of limestone and additives are same
4. Exhaust gas and atmospheric air is incompressible
5. Steady state conditions (Temperature is constant throughout the time at all the considered locations)
6. Pressure in the control volume (P) is assumed constant and as 101325 Pa
7. The composition of the inlet gas stream does not change much throughout the system. (i.e. the molecular weight of the gas stream would remain the same though-out the process)
8. The moisture content of the raw meal going out from the raw meal department is negligible ($x_{H_2O,\,RM,\,out} = 0$)
9. The temperature of the crushed raw materials going out from the coarse separator and the cyclone system is equal to the temperature of the gas stream leaving the cyclone system ($T_{RM,\,out} = T_{G,\,AFM\,out}$)
10. The temperature of the bypass gas stream ($T_{G,\,BP}$) is equal to the temperature of the inlet gas stream into the raw meal department ($T_{G,\,in}$)
11. Oxygen and moisture fractions of the gas stream in the bypass gas stream, gas stream into the AFM are equal to the inlet gas stream coming into the raw meal department (i.e. $y_{O_2,G,\,in} = y_{O_2,\,BP} = y_{O_2,\,AFM\,in}$ and $y_{H_2O,\,G,\,in} = y_{H_2O,\,BP} = y_{H_2O,\,AFM\,in}$)
12. Assumed that the energy inputs from the AFM motor and the Fans are directly transferred to the gas stream (There are possible losses which have not been considered)
13. In energy balance equations heat losses (Q_{loss}) interprets the heat losses related to the location only. (see Figure 4-2 for exact heat loss values at the locations)

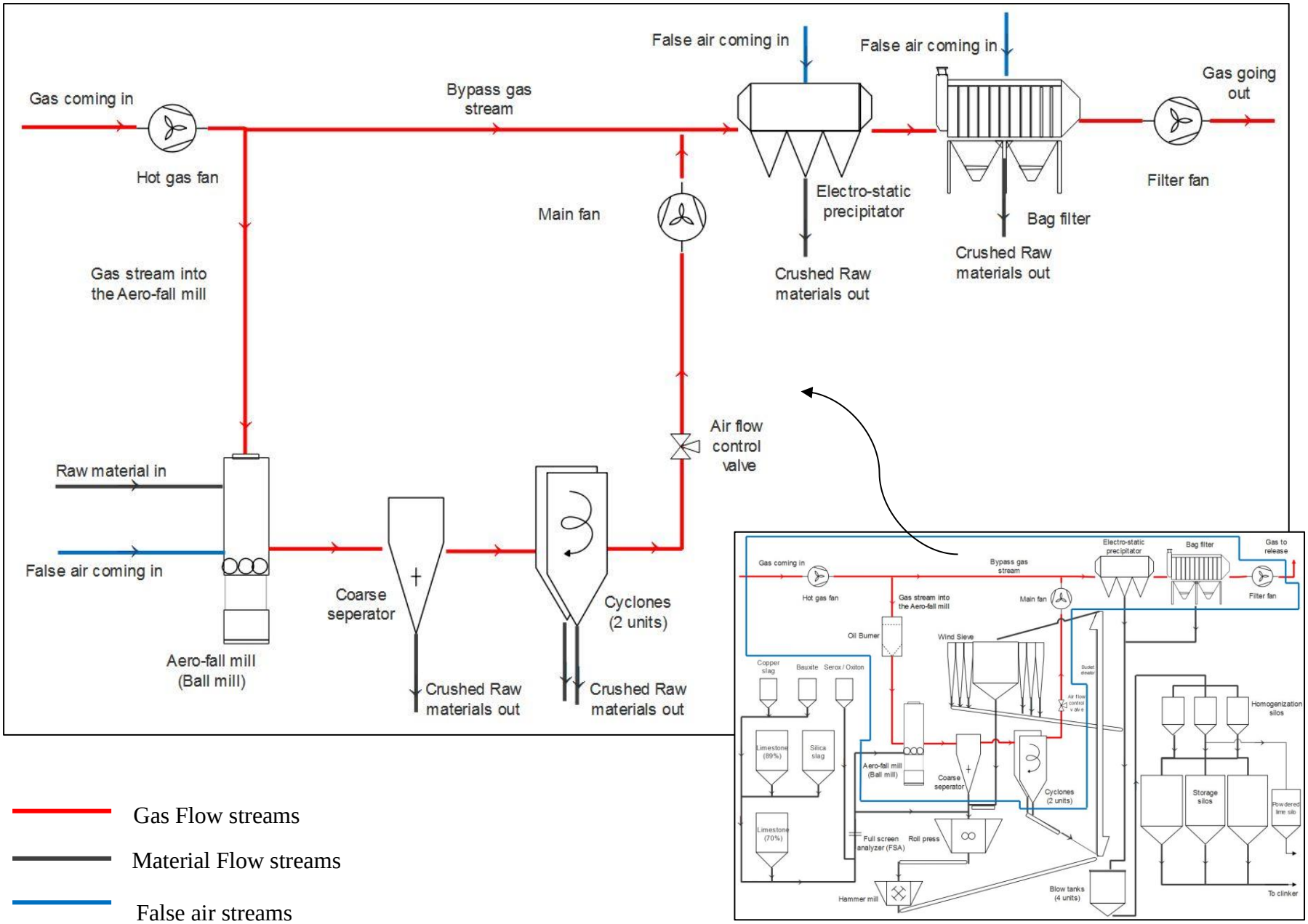

Figure 4-1: Control volume

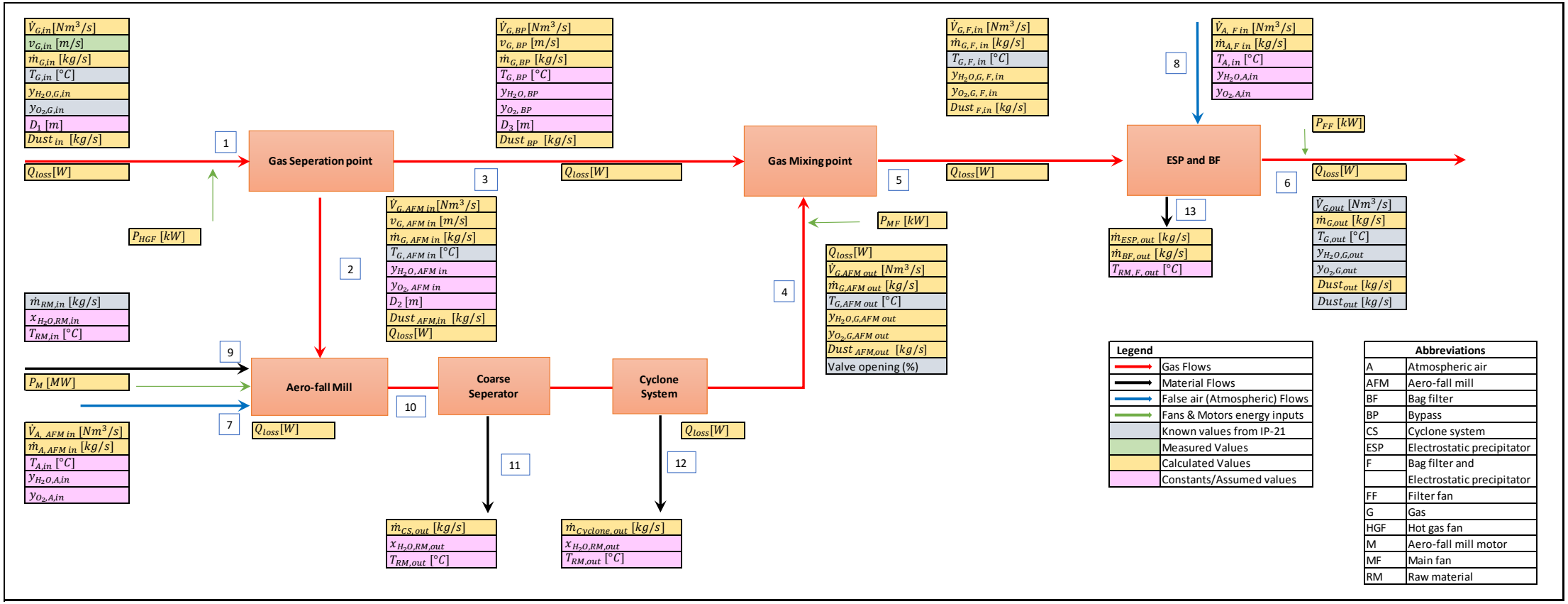

Figure 4-2: Block diagram of the control volume

4.2 Model

4.2.1 Mass balance

Mass balance for the gas stream at the gas separation point is given by equation (4.1) and mass balance for dust dissolved in the gas streams at gas separation point are given in equations (4.2)-(4.4).

$$\dot{m}_{G,\ in} = \dot{m}_{G,\ BP} + \dot{m}_{G,\ AFM\ in} \tag{4.1}$$

$$Dust_{\ in} = \frac{\dot{V}_{G,\ in} * C_{Dust,in}}{1000} \tag{4.2}$$

$$Dust_{\ BP} = Dust_{\ in} * \frac{\dot{m}_{G,\ BP}}{\dot{m}_{G,\ in}} \tag{4.3}$$

$$Dust_{AFM,\ in} = Dust_{\ in} - Dust_{\ BP} \tag{4.4}$$

The mass balance for the gas streams at the AFM, coarse separator, and the cyclone system is given by equation (4.5) and mass balance for the solid streams are given by equations (4.6)-(4.8).

$$\dot{m}_{G,\ AFM\ out} = \dot{m}_{G,\ AFM\ in} + \dot{m}_{A,\ AFM\ in} + \dot{m}_{RM,\ in} * x_{H_2O,RM,\ in} + Dust_{\ AFM,out} \tag{4.5}$$

$$\dot{m}_{CS,\ out} = [\dot{m}_{RM,\ in} * (1 - x_{H_2O,RM,\ in}) + Dust_{AFM,in}] * \eta_{CS} \tag{4.6}$$

$$\dot{m}_{Cyclone,\ out} = [\dot{m}_{RM,\ in} * (1 - x_{H_2O,RM,\ in}) + Dust_{AFM,in} - \dot{m}_{CS,\ out}] * \eta_{Cyclone} \tag{4.7}$$

$$Dust_{\ AFM,out} = [\dot{m}_{RM,\ in} * (1 - x_{H_2O,RM,\ in}) + Dust_{AFM,in} - \dot{m}_{CS,\ out} - \dot{m}_{Cyclone,\ out}] \tag{4.8}$$

Mass balance for the gas streams at the gas mixing point is shown in equation (4.9) and mass balance for dust dissolved in the gas stream at the gas mixing point is given in equation 4.10.

$$\dot{m}_{G,F,in} = \dot{m}_{G,\ BP} + \dot{m}_{G,\ AFM\ out} \tag{4.9}$$

$$Dust_{\ F,in} = Dust_{\ BP} + Dust_{\ AFM,out} \tag{4.10}$$

Mass balance for the gas and solid streams at the ESP and the BF is shown in equations (4.11)-(4.14).

$$\dot{m}_{G,\ out} + \dot{m}_{ESP,\ out} + \dot{m}_{BF,\ out} = \dot{m}_{G,F,in} + \dot{m}_{A,\ F\ in} \tag{4.11}$$

$$\dot{m}_{ESP,\ out} = Dust_{F,in} * \eta_{ESP} \quad (4.12)$$

$$\dot{m}_{BF,\ out} = (Dust_{F,in} - \dot{m}_{ESP,\ out}) * \eta_{BF} \quad (4.13)$$

$$Dust_{out} = (Dust_{F,in} - \dot{m}_{ESP,\ out} - \dot{m}_{BF,\ out}) \quad (4.14)$$

4.2.2 Component balance

Oxygen balance at the AFM, coarse separator, and the cyclone system is given in equation (4.15) and oxygen balance at the gas mixing point is given in the equation (4.16). Oxygen balance at the ESP and the BF is given in equation (4.17).

$$\dot{V}_{G,\ AFM\ out} * y_{O_2,\ G,AFM\ out} = \dot{V}_{G,\ AFM\ in} * y_{O_2,\ AFM\ in} + \dot{V}_{A,\ AFM\ in} * y_{O_2,A,in} \quad (4.15)$$

$$\dot{V}_{G,\ F,in} * y_{O_2,G,F,\ in} = \dot{V}_{G,\ BP} * y_{O_2,\ BP} + \dot{V}_{G,\ AFM\ out} * y_{O_2,\ G,AFM\ out} \quad (4.16)$$

$$\dot{V}_{G,\ out} * y_{O_2,G,\ out} = \dot{V}_{G,\ F,in} * y_{O_2,G,F,\ in} + \dot{V}_{A,\ F\ in} * y_{O_2,A,in} \quad (4.17)$$

Moisture (H_2O) balance at the gas mixing point is given in equation (4.18). Moisture balance at the ESP and the BF is given in equation (4.19).

$$\dot{V}_{G,\ F,in} * y_{H_2O,G,\ F,\ in} = \dot{V}_{G,\ BP} * y_{H_2O,\ BP} + \dot{V}_{G,\ AFM\ out} * y_{H_2O,G,AFM\ out} \quad (4.18)$$

$$\dot{V}_{G,\ out} * y_{H_2O,G,\ out} = \dot{V}_{G,\ F,in} * y_{H_2O,G,F,in} + \dot{V}_{A,\ F\ in} * y_{H_2O,A,\ in} \quad (4.19)$$

Moisture (H_2O) balance for the control volume around gas separation point, AFM, and gas mixing point (i.e. for stream numbers 1, 5, 7, 9, 11 and 12 as shown in Figure 4-2) is shown in equation (4.20).

$$\dot{V}_{G,\ in} * y_{H_2O,G,in} * \rho_{H_2O} + \dot{m}_{RM,\ in} * x_{H_2O,RM,\ in} + \dot{V}_{A,\ AFM\ in} * y_{H_2O,A,\ in} * \rho_{H_2O} = \dot{V}_{G,\ F\ in} * y_{H_2O,G,F,in} * \rho_{H_2O} + (\dot{m}_{CS,\ out} + \dot{m}_{Cyclone,\ out}) * x_{H_2O,RM,\ out} \quad (4.20)$$

4.2.3 Energy balance

Energy balance at the gas separation point is given by the equation (4.21) and energy balance for the gas streams at the gas mixing point is given by equation (4.22).

$$\dot{m}_{G,\ in} * Cp_G * T_{G,\ in} + P_{HGF} = \dot{m}_{G,\ BP} * Cp_G * T_{G,\ BP} + \dot{m}_{G,\ AFM\ in} * Cp_G * T_{G,\ AFM\ in} + Q_{loss} \quad (4.21)$$

$$\dot{m}_{G,F,in} * Cp_G * T_{G,\ F,\ in} = \dot{m}_{G,\ BP} * Cp_G * T_{G,\ BP} + P_{MF} + \dot{m}_{G,\ AFM\ out} * Cp_G * T_{G,\ AFM\ out} - Q_{loss} \quad (4.22)$$

Total energy balance for all the gas and mass streams at the AFM, coarse separator, and the cyclone system is given by the equation (4.27). The development of the equation (4.27) is shown by equations (4.23)-(4.26) where equation (4.23) shows the energy released by the hot gas stream, equation (4.24) shows the energy gained by the raw material, equation (4.25) shows the energy gained by the false atmospheric air and equation (4.26) shows the energy gained by the moisture in raw material mixture.

$$\dot{m}_{G,\ AFM\ in} * Cp_G * (T_{G,\ AFM\ in} - T_{G,\ AFM\ out}) \quad (4.23)$$

$$\dot{m}_{RM,\ out} * Cp_{RM} * (T_{RM,\ out} - T_{RM,\ in}) \quad (4.24)$$

$$\dot{m}_{A,\ AFM\ in} * Cp_A * (T_{G,\ AFM\ out} - T_{A,\ in}) \quad (4.25)$$

$$\dot{m}_{RM,\ in} * x_{H_2O,RM,\ in} * \left[L + Cp_{H_2O} * (T_{G,\ AFM\ out} - T_{RM,\ in})\right] \quad (4.26)$$

$$\dot{m}_{G,\ AFM\ in} * Cp_G * \left(T_{G,\ AFM\ in} - T_{G,\ AFM\ out}\right) + P_M = (\dot{m}_{CS,\ out} + \dot{m}_{Cyclone,\ out}) * Cp_{RM} * (T_{RM,\ out} - T_{RM,\ in}) + \dot{m}_{A,\ AFM\ in} * Cp_A * (T_{G,\ AFM\ out} - T_{A,\ in}) + \dot{m}_{RM,\ in} * x_{H_2O,RM,\ in} * \left[L + Cp_{H_2O} * \left(T_{G,\ AFM\ out} - T_{RM,\ in}\right)\right] + Q_{loss} \quad (4.27)$$

Energy balance for the gas streams at the ESP and the BF is given by the equation (4.28).

$$\dot{m}_{G,F,in} * Cp_G * T_{G,\ F,\ in} + \dot{m}_{A,\ F\ in} * Cp_A * T_{A,\ in} + P_{FF} = \dot{m}_{G,\ out} * Cp_G * T_{G,\ out} + (\dot{m}_{ESP,\ out} + \dot{m}_{BF,\ out}) * Cp_{RM} * T_{RM,\ F,\ out} + Q_{loss} \quad (4.28)$$

4.2.4 Mass flow rates

Normal flow rate conversion from velocities are given in equation (4.29)-(4.31) while mass flow rate conversion between normal flow rates are given in equation (4.32)-(4.39).

$$\dot{V}_{G,\ in} = \frac{\pi}{4} * {D_1}^2 * v_{G,\ in} * \frac{T_N * P}{T_{G,\ in} * P_N} \quad (4.29)$$

$$\dot{V}_{G,\ BP} = \frac{\pi}{4} * {D_3}^2 * v_{G,\ BP} * \frac{T_N * P}{T_{G,\ in} * P_N} \quad (4.30)$$

$$\dot{V}_{G,\ AFM\ in} = \frac{\pi}{4} * {D_2}^2 * v_{G,\ AFM\ in} * \frac{T_N * P}{T_{G,\ in} * P_N} \quad (4.31)$$

$$\dot{m}_{G,\ in} = \rho_G * \dot{V}_{G,\ in} \quad (4.32)$$

$$\dot{m}_{G,\ BP} = \rho_G * \dot{V}_{G,\ BP} \quad (4.33)$$

$$\dot{m}_{G,\ AFM\ in} = \rho_G * \dot{V}_{G,\ AFM\ in} \quad (4.34)$$

$$\dot{m}_{A,\ AFM\ in} = \rho_A * \dot{V}_{A,\ AFM\ in} \quad (4.35)$$

$$\dot{m}_{G,\ AFM\ out} = \rho_G * \dot{V}_{G,\ AFM\ out} \quad (4.36)$$

$$\dot{m}_{A,\ F\ in} = \rho_A * \dot{V}_{A,\ F\ in} \quad (4.37)$$

$$\dot{m}_{G,\ F\ in} = \rho_G * \dot{V}_{G,\ F\ in} \quad (4.38)$$

$$\dot{m}_{G,\ out} = \rho_G * \dot{V}_{G,\ out} \quad (4.39)$$

4.2.5 Parameters

Constant parameter calculation equations for density of gas, atmospheric air, and moisture (water vapor) at normal conditions are given in equation (4.40)-(4.42).

$$\rho_G = \frac{P_N * M_{wG}}{R * T_N} \quad (4.40)$$

$$\rho_A = \frac{P_N * M_{wA}}{R * T_N} \quad (4.41)$$

$$\rho_{H_2O} = \frac{P_N * M_{wH_2O}}{R * T_N} \quad (4.42)$$

4.2.6 Available heat

Available heat in the bypass gas stream respect to zero reference temperature is given in equation (4.43) where possible heat for LP steam generation and hot water generation from the available heat are given in equation (4.44) and (4.45) respectively.

$$Q = \dot{m}_{G,\ BP} * Cp_G * (T_{G,\ BP} - 0) \quad (4.43)$$

$$Q_{LP} = \dot{m}_{G,\ BP} * Cp_G * (T_{G,\ BP} - T_{ref1}) \quad (4.44)$$

$$Q_{HW} = \dot{m}_{G,\ BP} * Cp_G * (T_{ref1} - T_{ref2}) \quad (4.45)$$

In the model, there are 41 main equations with 38 total unknowns (variables + parameters) considering $v_{G,\ in}$ is measured and other parameters known from literature and plant process database. There are 3 extra equations to validate the results after the solving of the model.

5 Calculations

This chapter gives information about how the main model is solved, and the additional calculations done to support the main model. Moisture and dust concentration calculation of the inlet gas and heat loss estimations are among them. Possibility of LP steam and hot water production rate calculations along with yearly available heat at the conditioning tower are also calculated in this chapter. Calculation of lumped capacitance method for particles at the coarse separator and the cyclone system also performed in this chapter to validate an assumption made.

5.1 Model solving

The model was solved using Microsoft excel and by hand calculation. To solve the model several assumptions were made for some parameters and constant values. All the made assumptions are mentioned in subchapter 4.1.

A schematic back calculation from the exit gas stream to the inlet gas stream was conducted since most of the parameters from plant process database were available at the exit gas stream (stream 6 in Figure 4-2). Calculations were done when both Type HS and STD type are running in the AFM. The available heat was calculated for both scenarios with two end temperatures. Furthermore, the calculation was done when the AFM is not running. A summary of the main calculation is shown in Table 6-1.

A detail hand calculation for a Type HS scenario is shown in Appendix D and the solved block diagram for the same calculation is shown in Appendix B.

5.2 LP steam and hot water production from available heat

Specifications for available heat calculation and possible LP steam generation and hot water generation are shown in Table 5-1. Reasoning behind selecting values for end temperatures (T_{ref1} and T_{ref2}) are discussed in the subchapter 6.9. Equation (5.1) and (5.2) shows the equations that are used to calculate the possible production of LP steam ($\dot{m}_{steam}$) and hot water ($\dot{m}_{H_2O}$) from the available heat.

$$Q_{LP} * 10^3 = \dot{m}_{steam} * h_s(140\ °C) \tag{5.1}$$

$$Q_{HW} * 10^6 = \dot{m}_{H_2O} * Cp_{H_2O} * \left(T_{HW,\ out} - T_{HW,\ in}\right) \tag{5.2}$$

A detail calculation for possible LP steam and hot water generation is shown in Appendix E (for Type HS). Summary of the calculation results are given in Table 6-1.

Table 5-1: Specifications for LP steam and hot water production calculation

Parameter	Value	Units
T_{ref1}	130	$[°C]$
T_{ref2}	50	$[°C]$
Total specific enthalpy of steam ($h_s(140\ °C)$) [10]	2733	$[kJ/kg]$
Specific heat capacity of water (Cp_{H_2O}) [11]	4185	$[J/(kg.K)]$
Inlet temperature of the water used to generate hot water ($T_{HW,\ out}$)	0	$[°C]$
Temperature of the hot water generated ($T_{HW,\ in}$)	60	$[°C]$

5.3 Yearly heat availability at conditioning tower calculation when AFM is not running

When AFM is not running the loss of the heat is very significant at the conditioning tower because of added water. This available energy can be utilized if water is not added and the gas stream is bypassed through a couple of heat exchangers (For LP steam and hot water production). Heat availability, if conditioning tower is not operated when AFM is not running has been estimated using the specifications given in Table 5-2. Equation (5.3) and (5.4) has been used to calculate the average yearly available heat. Estimated available heat for LP steam and hot water generation are shown in Table 5-3.

$$Q_{LP,\ CT} = \dot{m}_{CT,in} * Cp_G * (T_{CT} - T_{ref1}) * t_{AFM\ downtime} * Weeks_{kiln} * 3600 \quad (5.3)$$

$$Q_{HW,\ CT} = \dot{m}_{CT,in} * Cp_G * (T_{ref1} - T_{ref2}) * t_{AFM\ downtime} * Weeks_{kiln} * 3600 \quad (5.4)$$

Table 5-2: Specifications for heat availability calculation at the conditioning tower when AFM is not running

Description	Value	Units
Average mass flow rate of hot gas via the conditioning tower when AFM is not running ($\dot{m}_{CT,in}$)	65	$[kg/s]$
Average gas temperature before the conditioning tower (T_{CT})	400	$[°C]$
Average heat capacity of gas ($Cp_G(T)$)	1150	$[W/kg/K]$
T_{ref1}	130	$[°C]$
T_{ref2}	50	$[°C]$
Assumed downtime of the AFM per week ($t_{AFM\ downtime}$)	15	$[h/week]$
No of kiln running weeks ($Weeks_{kiln}$)	48	$[weeks/yr]$

Table 5-3: Available heat at the conditioning tower when AFM is not running

Description	Value	Units
Estimated yearly average heat availability for LP steam at the conditioning tower when AFM is not running ($Q_{LP,\ CT}$)	52	$[TJ/yr]$
Estimated yearly average heat availability for Hot water at the conditioning tower when AFM is not running ($Q_{HW,\ CT}$)	16	$[TJ/yr]$

5.4 Moisture fraction estimation of the inlet gas stream

Using the main model the moisture content of the inlet gas coming into the raw meal department ($y_{H_2O,\,G,\,in}$) was calculated. Furthermore, moisture mass flow rate added at the conditioning tower was extracted from the data log system and then moisture fraction of the gas stream coming into the conditioning tower from the cyclone preheater towers ($y_{H_2O,CT,in}$) was estimated by using the equation (5.5)-(5.7). Specifications used for the calculation and results from the calculation are shown in Table 5-4.A detail calculation of inlet gas moisture estimation for Type HS is shown in Appendix F.

$$P_N * \dot{V}_{G,\ in} * y_{H_2O,\,G,\,in} = \frac{\dot{m}_{H_2O,in} * R * T_N}{M_{wH_2O}} \tag{5.5}$$

$$\dot{m}_{H_2O,CT,in} = \dot{m}_{H_2O,in} - \dot{m}_{H_2O,CT} \tag{5.6}$$

$$P_N * \dot{V}_{CT,in} * y_{H_2O,CT,in} = \frac{\dot{m}_{H_2O,CT,in} * R * T_N}{M_{wH_2O}} \tag{5.7}$$

Table 5-4: Specifications and results for the inlet gas moisture fraction estimation

Description	HS	STD	N/R	Units
Gas flow rate coming into the raw meal department ($\dot{V}_{G,\ in}$)	37.8	41.6	48.7	$[Nm^3/s]$
Water fraction of the inlet gas stream coming into the raw meal department ($y_{H_2O,\,G,\,in}$)	**11%**	**17.4%**	**12.4%**	[%]
Mass of water in the gas stream coming into the raw meal department ($\dot{m}_{H_2O,in}$)	3.40	5.8	4.9	$[kg/s]$
Water mass added at condition tower ($\dot{m}_{H_2O,CT}$)	0.93	3.68	3.11	$[kg/s]$
Gas flow rate coming into the conditioning tower ($\dot{V}_{CT,in}$)	37.1	39.0	46.4	$[Nm^3/s]$
Water mass coming into the conditioning tower with the gas stream ($\dot{m}_{H_2O,CT,in}$)	2.5	2.1	1.8	$[kg/s]$
Water/moisture fraction of the gas stream coming into the conditioning tower ($y_{H_2O,CT,in}$)	**8.3%**	**6.8%**	**4.8%**	[%]

5.5 Inlet gas dust concentration estimation

Dust flow rate along with the inlet gas stream into the raw meal department ($Dust_{in}$) was unknown. When the gas stream going through the preheater tower cyclone system before the raw meal department, it carries a small fraction of raw meal feed that feed into the preheater towers. There are two cyclone towers to preheat the raw meal before sending them to the pre-calciner. Only the gas stream going through the cyclone tower number 2 is sent to the raw meal department. The gas stream is passed via an ESP followed by a conditioning tower as shown in Figure 2-15.

Equation (5.8)-(5.10) were used to estimate the inlet gas dust concentration, $C_{Dust,in}$. Assumed dust/gas separation equipment efficiencies are shown on Table 5-5. Inlet duct concentration was estimated as shown in Table 5-6. A detail calculation of the calculation is given in Appendix C.

Since inlet dust concentration ($C_{Dust,in}$) is estimated as 3 g/Nm^3, $Dust_{in}$ can be calculated according to the inlet gas velocity, $\dot{V}_{G,\ in}$ as shown in equation 4.2.

$$Dust_{tower,\ out} = \dot{m}_{RM,\ tower,\ in} * \left(1 - \eta_{Cyclone}\right) \quad (5.8)$$

$$Dust_{ESP3,\ out} = Dust_{tower,\ out} * (1 - \eta_{ESP}) \quad (5.9)$$

$$C_{Dust,in} = \frac{Dust_{ESP3,\ out} * 10^6}{\dot{V}_{G,\ in}} \quad (5.10)$$

Table 5-5: Assumed dust/gas separation equipment efficiencies

Equipment	Efficiency
Cyclone tower/system ($\eta_{Cyclone}$)	90%
ESP (η_{ESP})	95%
BF (η_{BF})	99%
Coarse separator (η_{CS})	70%

Table 5-6: Inlet gas dust concentration calculation

Description	Value	Unit
Raw meal into cyclone tower number 2 (preheating tower) ($\dot{m}_{RM,\ tower,\ in}$)	115	$[t/h]$
Dust mass flow rate coming out from the cyclone tower (preheating tower) along with the hot gas stream ($Dust_{tower,\ out}$)	11.5	$[t/h]$
Dust mass flow rate coming out from the ESP (no.3) along with the hot gas stream ($Dust_{ESP3,\ out}$)	0.575	$[t/h]$
Average hot gas flow rate into the raw meal department (measured at the calculated moment) ($\dot{V}_{G,\ in}$)	190000	$[Nm^3/h]$
Dust concentration in the hot gas stream ($C_{Dust,in}$)	**3**	$[g/Nm^3]$

5.6 Heat loss estimation

There is a heat loss from pipelines and equipment which is significant at some locations. At some locations heat loss is negligible. To estimate the heat losses, average surface areas of the equipment and pipelines were estimated. Since surface temperature of the were measured and averaged, using equation (5.11) average heat losses were estimated (see Table 5-8). Values in Table 5-7 were assumed for the heat loss estimation.

Table 5-7: Assumed parameters for heat loss estimation

Parameter	Value	Units
Outside temperature ($T_{A,\ in}$)	5	[$°C$]
Average overall heat transfer coefficient (U) [12]	10	[$W/m^2/K$]

$$Q_{loss} = U * A_{sur} * (T_{sur} - T_{A,\ in})/1000 \quad (5.11)$$

Table 5-8: Heat loss estimation at pipelines and process equipment

Location	Surface area (A_{sur}) (m^2)	Average temperature (T_{sur}) (°C)	Average heat loss (Q_{loss}) (kW)
At inlet pipe (stream 1)	68	31	18
Towards AFM (stream 2)	20	30	5
Bypass line (stream 3)	79	34	23
Before AFM	32	89	27
At AFM	126	29	30
At two cyclones	265	40	94
Inlet and outlet pipes of cyclones	36	31	9
Before gas mixing, from AFM	14	53	7
To outside line (after gas mixing and before ESP)	68	99	64
At ESP and BF	-	-	100 (Assumed)
Total estimated heat loss (kW)			**376**

5.7 Lumped capacitance method

In the model assumptions (subchapter 4.1), it has stated that the temperature of the crushed raw materials going out from the coarse separator and cyclone system ($T_{RM,\ out}$) are same as the gas temperature that going out from the cyclone system ($T_{G,\ AFM\ out}$). This assumption can be validated by applying the lumped capacitance method at the coarse separator and cyclone systems.

Following assumptions have been made to execute the lumped capacitance method calculation.

1. The temperature of the solid inside the coarse separator and the cyclone system is assumed spatially uniform
2. The temperature inside the coarse separator and the cyclone system is a function of time only. i.e. $T = T(t)$
3. Particles shape is spherical after the raw materials are crushed from the AFM

Considering the transient condition energy balance the residence time of the particle is given by the equation (5.12) [13].

$$t_f = \tau * ln\left[\frac{T_i - T_\infty}{T_f - T_\infty}\right] \tag{5.12}$$

Where thermal time constant (τ) is given by the (5.13).

$$\tau = R_t * C_t \tag{5.13}$$

Thermal capacitance (C_t) and convection thermal resistance (R_t) is given by equation (5.14) and (5.15).

$$C_t = \rho * V * Cp_{RM} \tag{5.14}$$

$$R_t = \frac{1}{h * A_s} \tag{5.15}$$

Equation (5.12) can be expanded to equation (5.16).

$$t_f = \frac{\rho_{RM} * Cp_{RM} * D_p}{6 * h} * ln\left[\frac{T_i - T_\infty}{T_f - T_\infty}\right] \tag{5.16}$$

The lumped capacitance method is valid only if Biot number is very small to one. i.e. $Bi \ll 1$

Biot number is given by the equation (5.17).

$$Bi = \frac{h * L_c}{k} \tag{5.17}$$

Where, Characteristic length (L_c) of the particles is given by equation (5.18).

$$L_c = \frac{V}{A_s} \tag{5.18}$$

Specifications that used for the lumped capacitance method are shown in Table 5-9 and results obtained from the calculation are shown in Table 5-10. A detail calculation is shown in Appendix G.

Table 5-9: Specifications for the lumped capacitance method calculation

Symbol	Value	Units
D_p	9*10^{-5}	$[m]$
k	1.3	$[W/m^2/K]$
h	30	$[W/m^2/K]$
ρ_{RM}	1522	$[kg/m^3]$
Cp_{RM}	910	$[J/kg/K\ ]$
T_i	15	$[°C]$
T_f	65.5	$[°C]$
T_∞	164.25	$[°C]$

Table 5-10: Results from the lumped capacitance method calculation

Symbol	Value	Units
Bi	0.00034	$[-]$
τ	5.2*10^{-7}	$[s]$
t_f	0.286	$[s]$

6 Results and Discussion

In this chapter, the results generated from the main model and supplementary calculations are discussed. Mainly the available heat at bypass gas for different process types are interpreted and discussed. Furthermore, different paraments that might affect the heat availability are discussed along the bypass line. A special attention has been given to discuss the differences in temperatures and gas flows inside the raw meal department for different process conditions. Also, made assumptions has been discussed in this chapter along with model validation results. The possibility of heat recovery at the conditioning tower when AFM is not running is also been discussed. In addition, several process related aspects such as possibility of gas backflow via the bypass line, the false air coming into the system, reasons for selection of the end temperatures of heat recovery and practical issues with heat recovery are being discussed in this chapter.

6.1 Waste heat availability in the bypass line and Heat flow interpretation

Table 6-1 shows the summary of main calculation that relates to the heat availability at the bypass line. It does show how much heat is available for LP steam generations and hot water generation for each process conditions. Furthermore, Table 6-1 shows the possible mass flow rates of LP steam and hot water that can be generated from the available heat.

Table 6-1: Summary of the main calculation

Description	Type HS	STD Type	Not running (N/R)	Units
Valve opening	36	66	0	[%]
Gas flow rate into the AFM ($\dot{V}_{G,\ AFM\ in}$)	18	23	0	$[Nm^3/s]$
Bypass line flow rate ($\dot{V}_{G,\ BP}$)	20	18	48	$[Nm^3/s]$
Bypass line mass flow ($\dot{m}_{G,\ BP}$)	28	25	67	$[kg/s]$
Bypass line temperature ($T_{G,\ BP}$)	266	185	185	$[°C]$
Heat availability (ref 0 °C) (Q)	**8.2**	**5**	**13.4**	$[MW]$
LP Steam (end temperature 130 °C) (Q_{HW})	**4.2**	**1.5**	**4**	$[MW]$
Steam generation ($\dot{m}_{steam}$)	**1.5**	**0.5**	**1.5**	$[kg/s]$
Hot water (130 °C - 50 °C) (Q_{LP})	**2.5**	**2.2**	**5.8**	$[MW]$
Hot water generation ($\dot{m}_{H_2O}$)	**9.8**	**8.4**	**22.6**	$[kg]$

Figure 6-1 shows the graphical representation for available heat for different process conditions while Figure 6-2 shows the graphical representation for possible LP steam generation and Hot water generation from the available heat.

There is a high heat availability to produce LP steam when Type HS is running and when AFM is not running (4.2 MW and 4 MW respectively). There is more heat available (5.8 MW) to generate hot water. The heat available to generate hot water is approximately similar when Type HS and STD type is running (2.5 MW and 2.2 MW respectively).

When it comes to the production of LP steam and hot water at the bypass line, STD type has the lowest LP steam production rate (0.5 kg/s) because the inlet gas temperature is lower (around 180 °C). The production of hot water rate is very high (22.6 kg/s) when AFM is not running since there is a higher mass flow rate of the hot gas present with sensible heat inside the bypass line even though the gas temperature is around 180 °C.

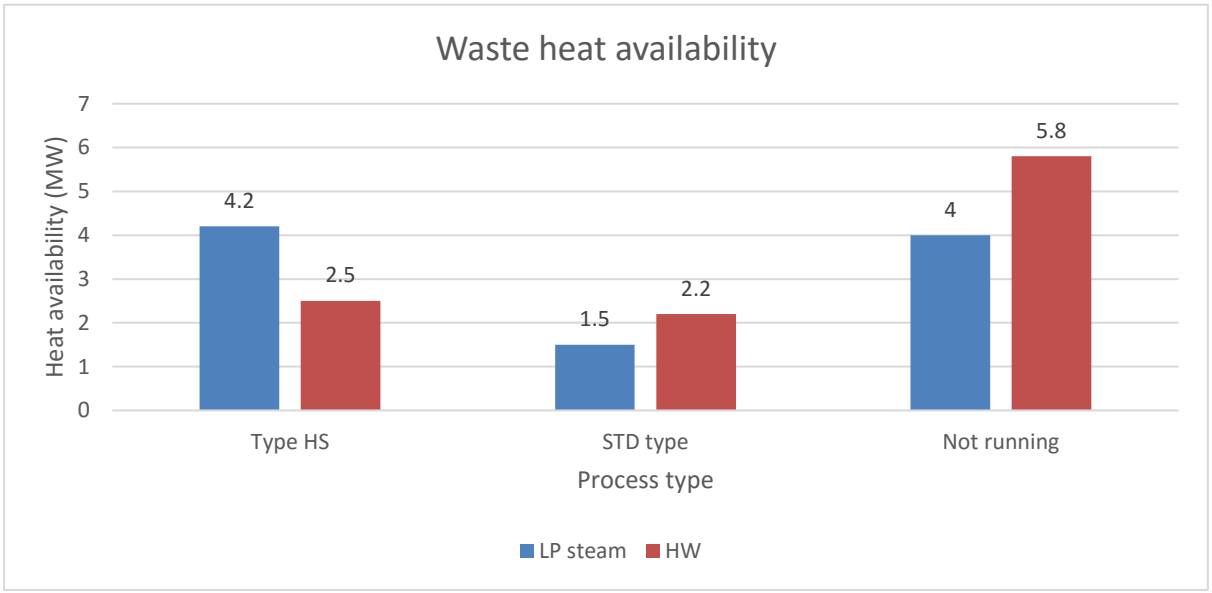

Figure 6-1: Waste heat availability for different process conditions

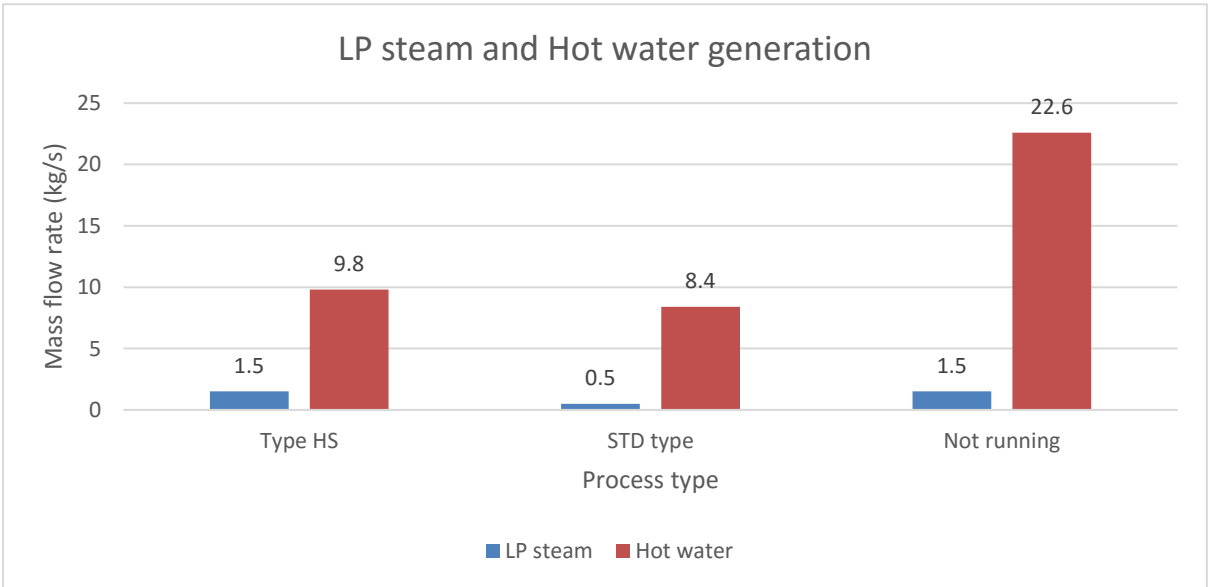

Figure 6-2: Possible LP steam generation and Hot water generation from the available heat

Furthermore, Heat flows have been interpreted using the Sankey diagrams for Type HS, STD type and when AFM is not running. For each case both heat flows with and without heat recovery has been shown. All the heat flows for gas streams, raw material streams, power inputs from the fans and AFM Motor along with estimated heat losses are shown in the Sankey figures. All the heat flows are interpreted to 0 °C reference temperature. All the Sankey diagrams that are shown below are in the same scale.

Figure 6-3 shows the heat flows for the Type HS without any heat recovery where Figure 6-4 shows the heat flows for Type HS with possible heat recovery via the bypass gas line.

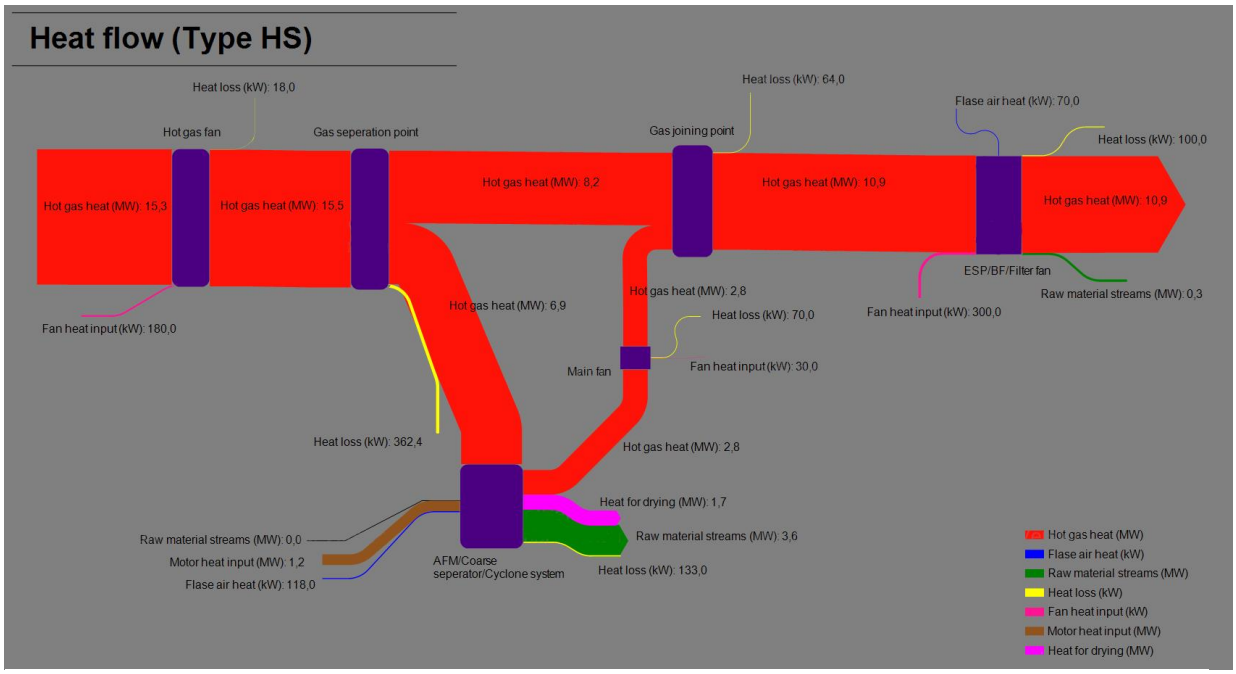

Figure 6-3: Sankey diagram for the heat flows when Type HS is running

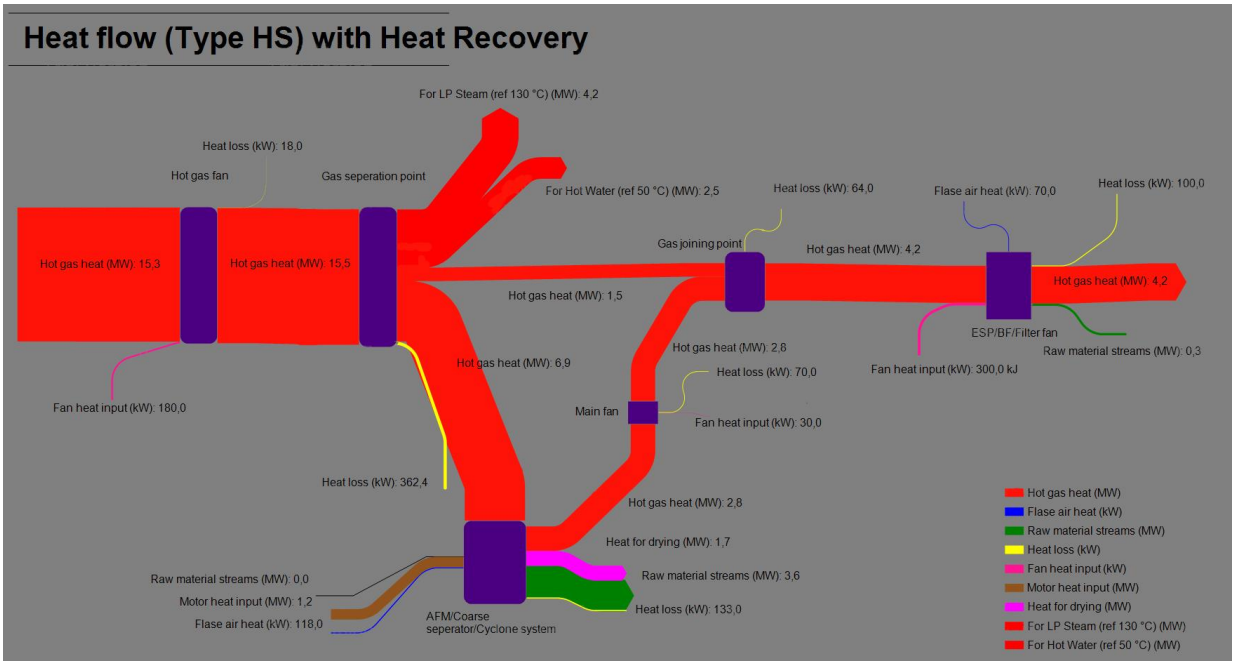

Figure 6-4: Sankey diagram for the heat flows with possible heat recovery when Type HS is running

Figure 6-5 shows the heat flows for the STD type without any heat recovery where Figure 6-6 shows the heat flows for STD type with possible heat recovery via the bypass gas line.

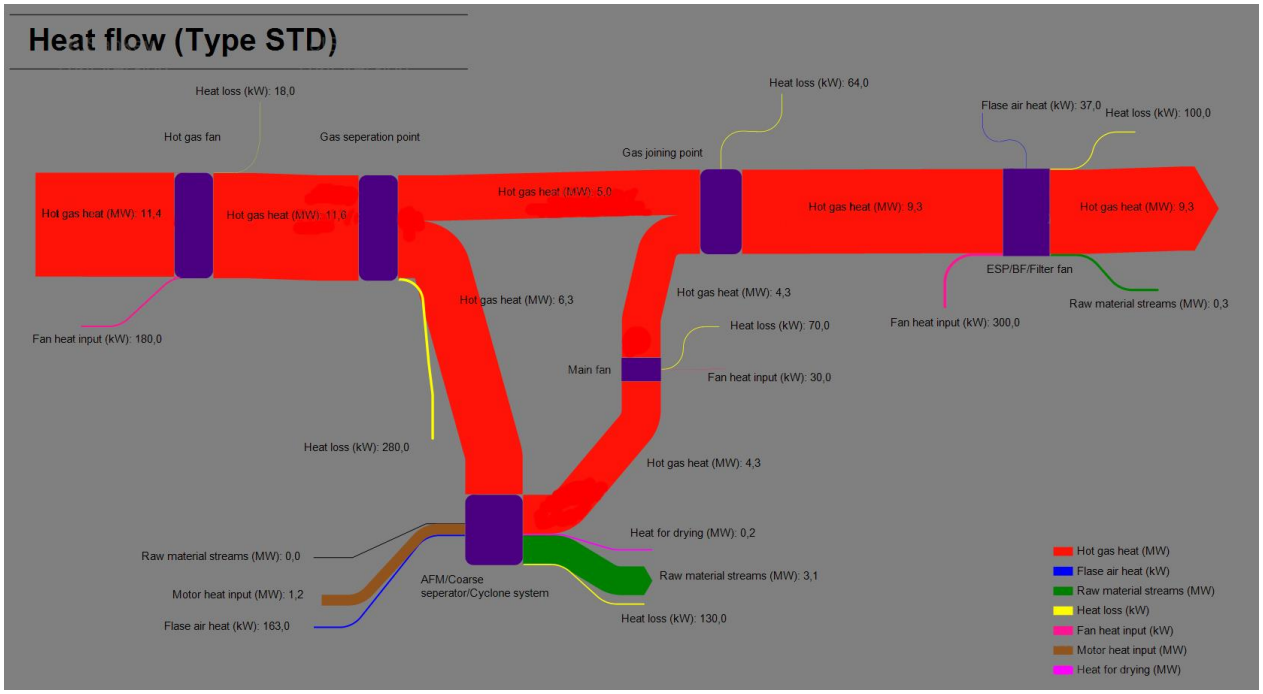

Figure 6-5: Sankey diagram for the heat flows when STD type is running

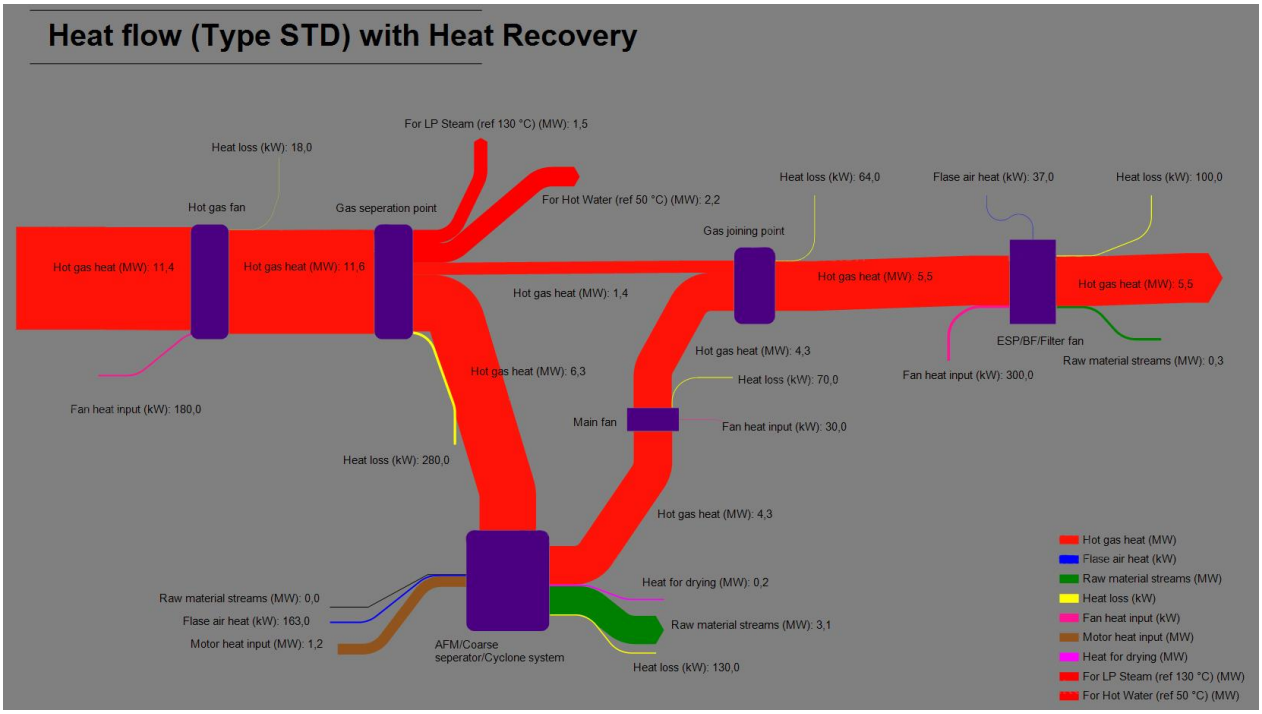

Figure 6-6: Sankey diagram for the heat flows with possible heat recovery when STD type is running

When the AFM is not running all the hot gas coming into the raw meal department is sent via the bypass line. Figure 6-7 shows the heat flow when AFM is not running where Figure 6-8 shows the heat flows with possible heat recovery.

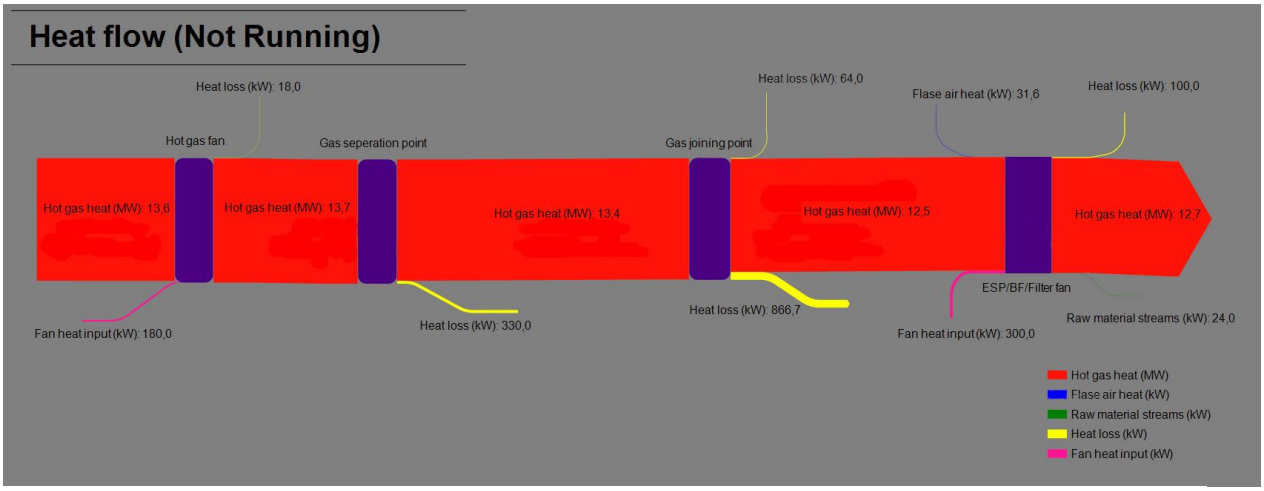

Figure 6-7: Sankey diagram for the heat flows when AFM is not running

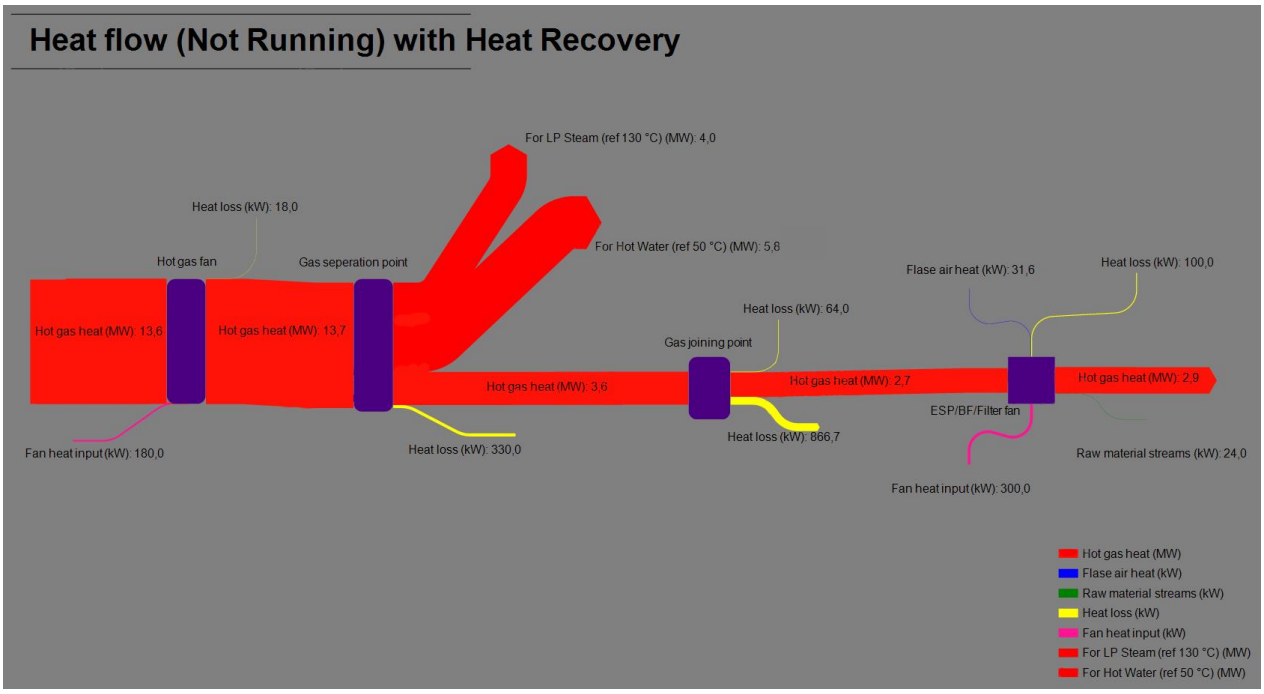

Figure 6-8: Sankey diagram for the heat flows with possible heat recovery when AFM is not running

6.2 Analyzing parameter profiles along the bypass line (before heat recovery)

6.2.1 Temperature and gas flow rate profiles along the bypass line

Figure 6-9 shows the temperature profile along the bypass line. In plant process database, a temperature sensor in the bypass gas stream was not available. To solve the model and to calculate the available heat, knowing the bypass gas stream temperature was critical. So, it has been assumed the temperature of the bypass gas stream ($T_{G,\ BP}$) is equal to the temperature of the inlet gas stream into the raw meal department ($T_{G,\ in}$). The distance from the temperature sensor of the inlet gas stream to the bypass line is about 5 m and there are no obstacles along the gas stream inside the pipelines. So, a temperature reduction of the gas stream up to the bypass line from the inlet line temperature sensor is hard to expect since the pipelines are properly insulated. So, the temperature inside the bypass line remain almost same as the inlet gas for Type HS and STD type as shown in Figure 6-9. Reasoning behind the temperature difference in inlet gas stream for different process conditions are explained in subchapter 6.3 and 6.7.

After the gas stream from bypass line and gas stream coming from the cyclone system mixed, there is a reduction of gas temperatures since the gas stream coming from the cyclone system carries a low sensible heat.

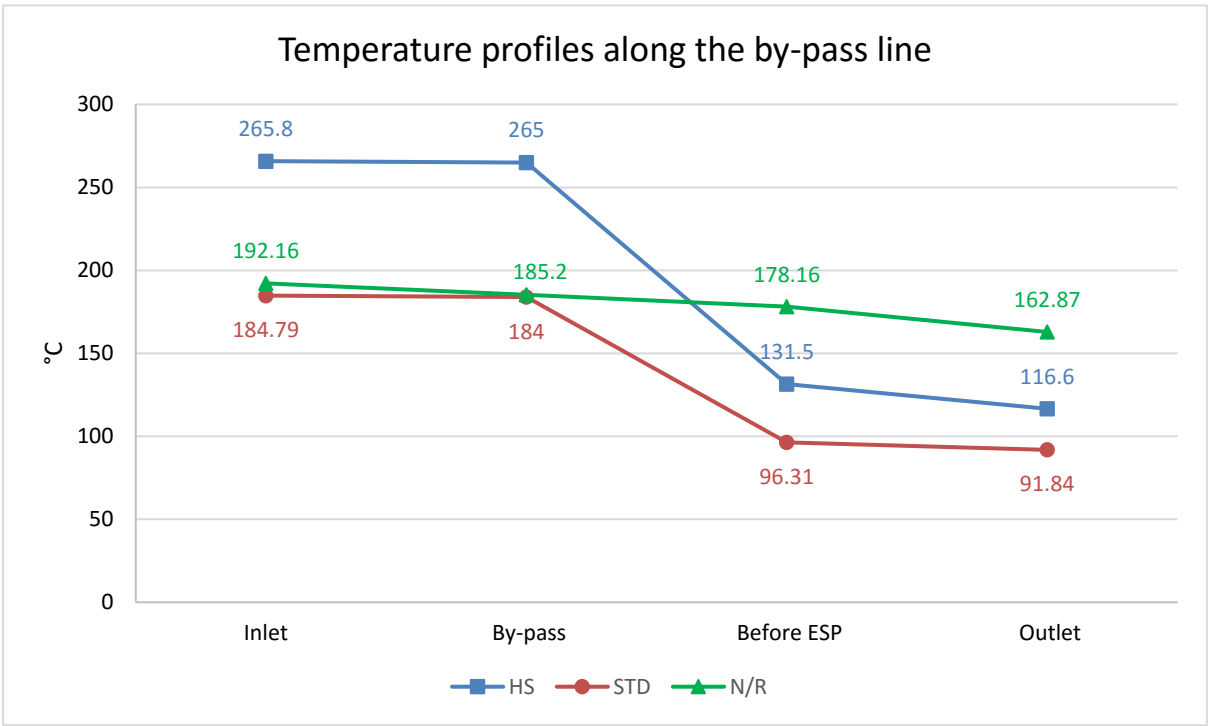

Figure 6-9: Temperature profiles along the bypass line

When AFM is not running, a fraction of inlet gas stream goes inside to the burner (a valve closes the gas stream just before the AFM when AFM is not running) and some gas stream is going towards to the main fan via gas mixing point. Hence a considerable temperature gradient in between inlet gas stream and gas stream after the mixing point can be observed. Heat loss through the burner and gas backflow via the fan shafts is the probable explanation for this

temperature gradient. So, when AFM is not running estimating of the bypass gas line temperature was done by taking the average temperature between inlet gas stream ($T_{G,\ in}$) and the temperature of the gas stream after the gas mixing ($T_{G,\ F,\ in}$).

The gas temperature reduction at the outlet compared to the gas temperature before ESP is just due to the false air coming into the system via AFM and BF. Furthermore, dust streams going out from the ESP and the BF also carries some sensible heat.

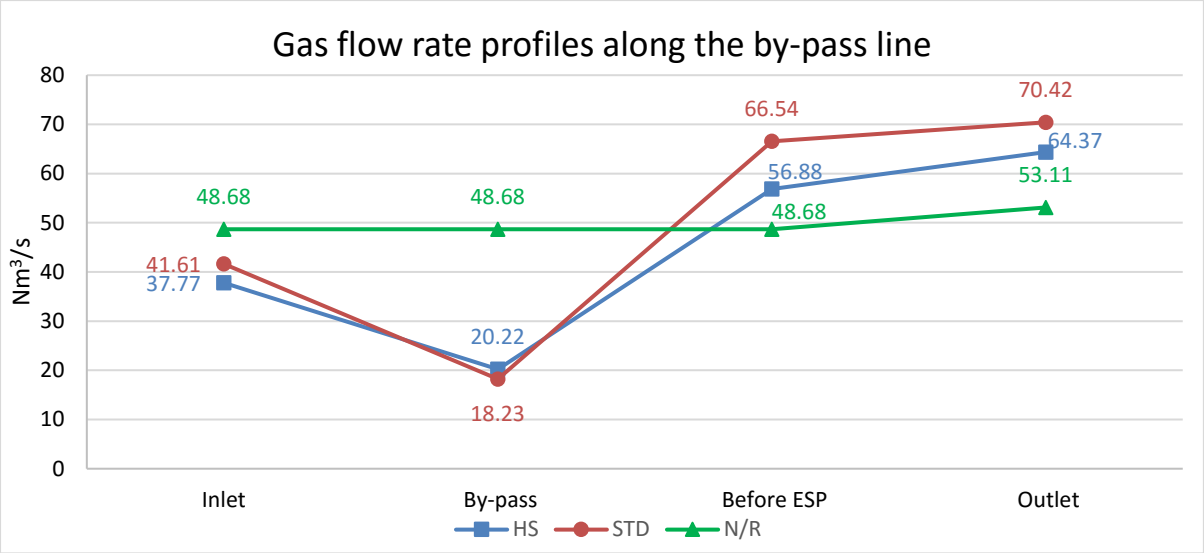

Figure 6-10: Gas flow rate profiles along the bypass line

Gas flow rate profiles along the bypass line are shown in Figure 6-10. The sudden drop of gas flow rate inside the bypass line is due to the fraction of the gas stream is sent via the AFM. Then there is an increment of gas flow rate after the gas mixing point along with some additional air. This is due to the false air induction at the AFM. Further gas flow rate keeps increasing due to the false air induction into the system from ESP and the BF.

The main parameters that directly affect the heat availability at the bypass gas stream are gas mass flow rate and gas temperature. It was hard to observe the variation of inlet gas mass flow rate over a time due to the unavailability of gas flow rate data at the gas inlet. But it can be assumed that the gas mass flow rate via the bypass line do change according to the hot gas requirement at the AFM. It has been observed that the gas temperature of the inlet gas stream fluctuates ±5°C during the stable process conditions. So, a slight negligible variation of heat availability at the bypass gas stream can be expected.

6.2.2 Moisture and Oxygen mole fraction profiles along the bypass line

Figure 6-11 shows the mole fraction of moisture along the bypass line while Figure 6-12 shows the mole fraction of oxygen along the bypass line.

Inlet gas stream does contain moisture content which is gained from waste fuel (pre-calciner and the kiln in Norcem Brevik use waste fuels as a heating source) and from the conditioning tower. As per the calculation is done in subchapter 5.4 the moisture content of the gas stream coming into the conditioning tower ($y_{H_2O,CT,in}$) lies around 4% to 8%. Rest of the moisture is from the added water at the conditioning tower. The amount of water added at the conditioning tower depends on regulating the inlet gas temperature ($T_{G,\ in}$) (further discussed in subchapter

6.3). Meanwhile, the oxygen fraction of the inlet gas varies around 7% to 8.5%. This oxygen is coming probably from the unburned oxygen of the kiln gas.

When gas stream is separated into two gas streams, the bypass line and the gas stream into the AFM, the gas streams does not affect by any false air. So, the assumption made to consider the moisture and oxygen fraction remain same in the inlet gas stream and the bypass gas stream is reasonable.

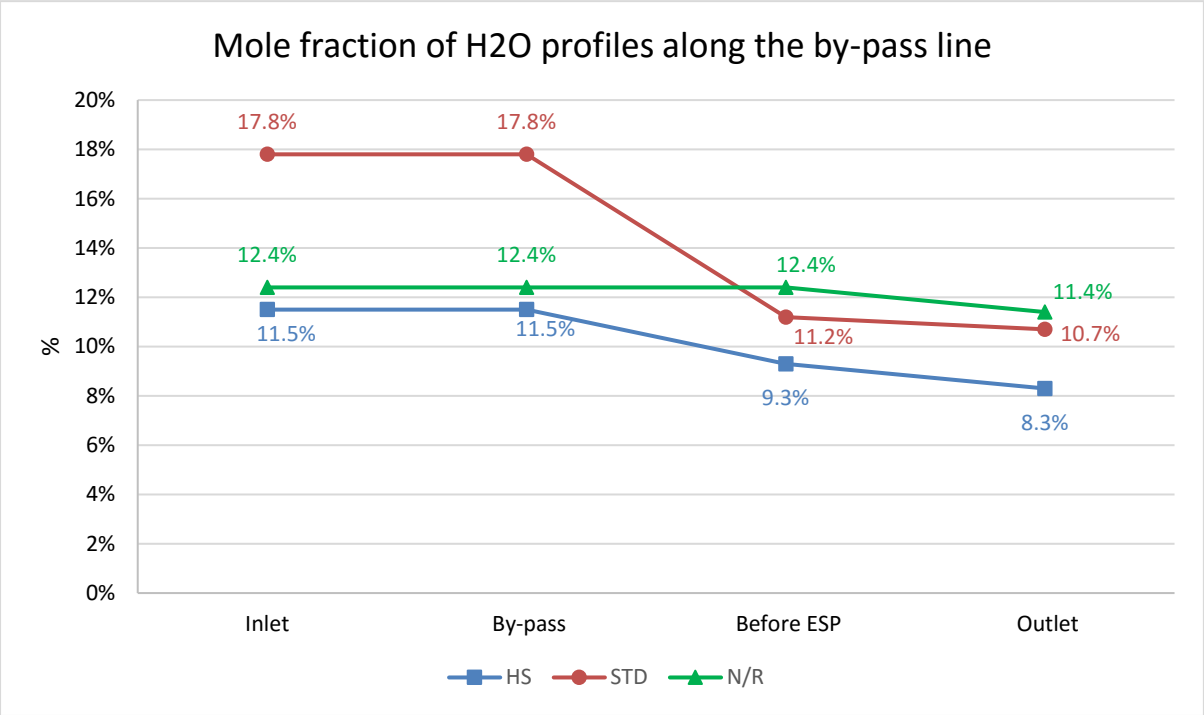

Figure 6-11: H_2O mole fraction profiles along the bypass line

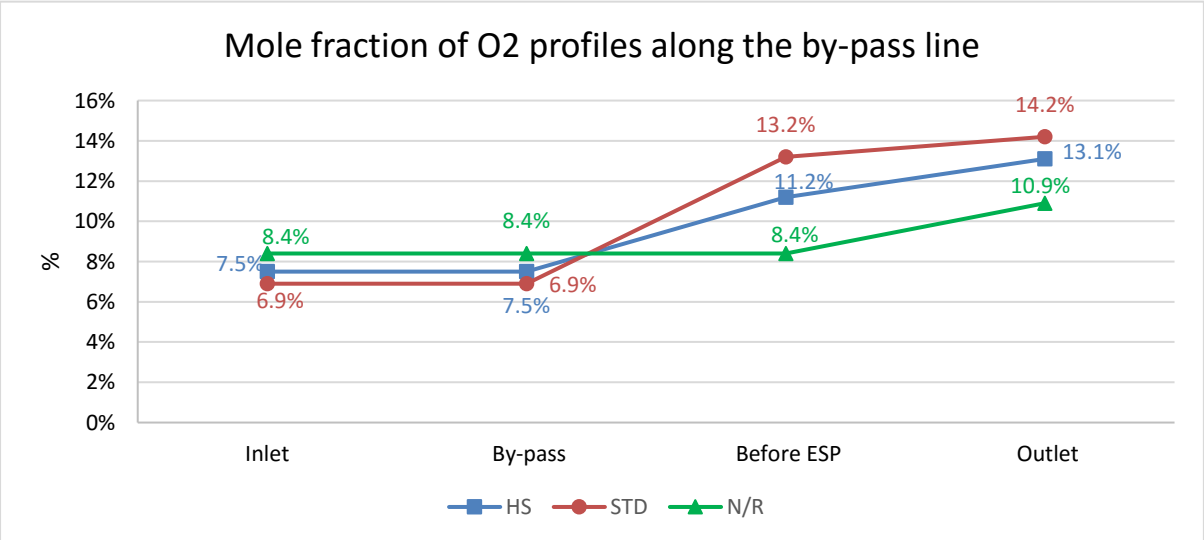

Figure 6-12: O_2 mole fraction profiles along the bypass line

There is a reduction of moisture fraction and increment of oxygen fraction just after the gas mixing point. The moisture fraction does reduce further at the outlet gas stream and oxygen

fraction does keep increasing. The false air induced into the raw meal department via the AFM, ESP and the BF is the reason for this phenomenon.

There is some amount of moisture is added to the gas stream during the drying process at the AFM. But the overall moisture fraction reduces due to the increment of gas flow rate from false air induction. Furthermore, false air does contain less fraction of moisture compared to the main gas stream, hence overall moisture fraction reduces. Since, atmospheric air contains 0.21% oxygen, the overall oxygen fraction of the gas streams keep increasing.

When AFM is not running, moisture and oxygen compositions remain almost the same except at the outlet gas stream because false air affects only at the ESP and the BF.

6.2.3 Dust mass flow rate profiles along the bypass line

Figure 6-13 shows the dust mass flow rates along the bypass line. Inlet gas does have a fraction of dust stream since it comes via the preheater towers (see subchapter 5.5 for more explanation). The dust flow rate inside the bypass line is significantly important when it`s come to the heat recovery because there can be issues with dust accumulation. The dust flow rate inside the bypass line is higher when AFM is not running compared to Type HS and STD type just because all the gas stream goes via the bypass gas stream.

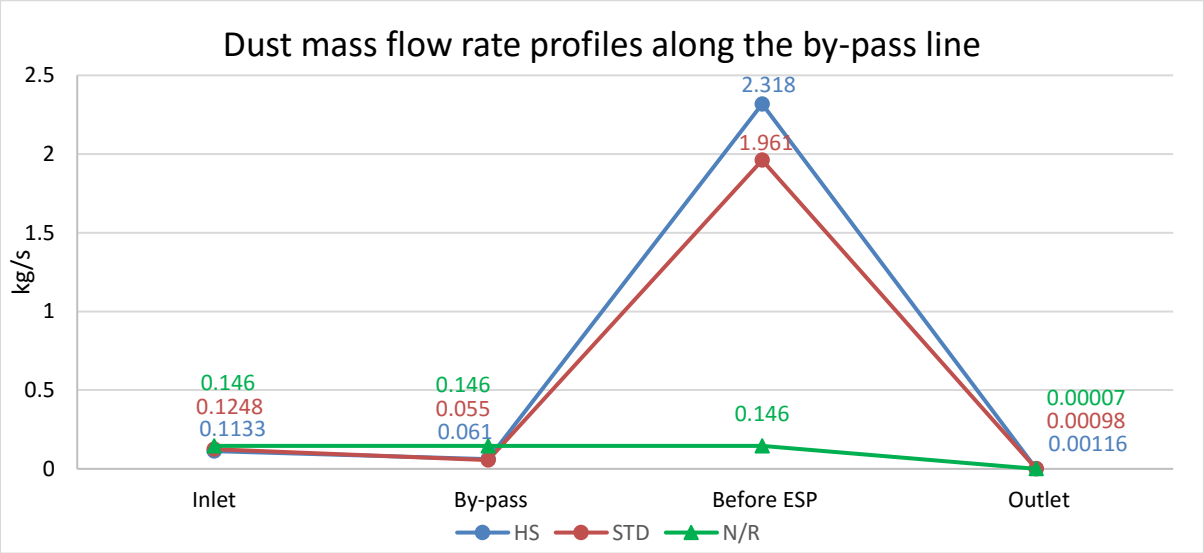

Figure 6-13: Dust mass flow rate profiles along the bypass line

The ratio of the heat carrying capacity by the dust stream inside the bypass line to the heat carrying capacity by the total gas stream inside the bypass line (X_{Dust}) can be expressed using the equation (6.1). As shown in Table 6-2 dust heat carrying capacity per unit gas of mass of is a very low value (0.002) for all the process conditions. This implies the mass flow rate of dust in the gas stream does not influence the total heat availability in the bypass gas stream.

$$X_{Dust} = \frac{Dust_{BP} * Cp_{RM}}{\dot{m}_{G,\,BP} * Cp_G} \tag{6.1}$$

Table 6-2: Heat carrying capacity analysis of dust inside the bypass line

Process Type	X_{Dust}
Type HS	0.002
STD type	0.002
AFM not running	0.002

There is a significant dust mass flow rate increment before the ESP (After gas mixing point). This is because the gas stream coming from the cyclone system carries a significant mass of dust (crushed raw materials) which are unseparated. Since dust is almost completely removed from the ESP and BF the gas stream released to the atmosphere is almost free with dust.

6.3 Reasoning for gas flow rate and temperature differences for Type HS and STD type inside the control volume

Type STD raw material recipe do contain typically 45% of high-quality limestone from Dalen mine and Verdal mine and 50% of low-quality limestone from Bjorntvet quarry while Type HS raw material recipe typically does contain only 84% of high quality limestone from Dalen mine and Verdal mine as the limestone source (See Table 2-1).

The hardness of the limestone from Bjorntvet quarry is higher compared to the limestone from Dalen mine and Verdal mine. Which implies limestone from Bjorntvet quarry need more crushing power and time at the AFM. But the balls inside AFM will fail in the long run if Bjorntvet limestone is kept inside the AFM for a long time. So, when STD type is running (STD type contain more limestone from Bjorntvet quarry) crushed raw materials is need to be taken out from the AFM in quick time and send to the roller press to do the further crushing. Roller press can crush the Bjorntvet limestone efficiently without making any wear in the equipment. A higher gas flow rate is sent via the AFM by increasing the valve opening when STD type is running to achieve this phenomenon. A lower valve opening is used when HS type is running. If a higher valve opening is used when Type HS is running more crushed materials will go out from the AFM and it might overload the roller press. Keeping Type HS raw meal mixture for a longer time inside AFM will not affect the balls since Dalen mine and Verdal mine limestone is easy to crush). Average valve openings are shown in 1st row of Table 6-1. (See Figure 2-8 for valve location)

Furthermore, when STD type is running inlet gas temperature is maintained around 180 °C while Type HS is running the gas temperature is maintained around 260 °C. The temperature of the gas stream is regulated in a scrubbing tower by adding water to the gas stream just before the gas stream enter to the raw meal department (see Figure 2-15). The moisture content in Verdal mine limestone, quarts and serox are relatively high compared to the moisture content in the limestone coming from Bjorntvet quarry and other additives. Since Type HS includes a higher fraction of Verdal mine limestone, quarts and serox (see Table 2-1), a higher gas temperature is required to dry the raw materials at the AFM.

Heat load sent to the AFM when Type HS and STD type is running were investigated per unit raw material feed (see Table 6-3). Equation (6.2) was used to calculate $Q_{AFM,in}$value to get

results in Table 6-3 calculation. According to the results heat load per unit raw material ($Q_{AFM,in}/\dot{m}_{RM,\ in}$) is 90 kJ/kg for Type HS and 99 kJ/kg for STD type. It seems the heat load per unit raw material is relatively similar for both type even though different temperatures are maintained in the gas streams.

$$Q_{AFM,in} = \dot{m}_{G,\ AFM\ in} * Cp_G * (T_{G,\ AFM\ in} - 0) \tag{6.2}$$

Table 6-3: Heat load sent to the AFM per unit mass of raw material for different process conditions

Process Type	**Heat load sent to the AFM per unit mass of raw material ($Q_{AFM,in}/\dot{m}_{RM,\ in}$) - ($kJ/kg$)**
Type HS	90
STD type	99

When gas temperature is reduced at the conditioning tower the gas flow rate reduces to maintain the same mass flow rate [$\dot{V}_{G,\ in} \propto T_{G,\ in}$]. Since more air flow rate is required when STD type is running to compensate the reduced air flow rate, more valve opening is required to have more air into the AFM.

The fan located after the conditioning tower (see Figure 2-15) do work more efficiently when the gas temperature is around 180 °C. This is another reason the gas temperature is kept around 180 °C when STD type is running and when AFM is not running. (Discussed further in subchapter 6.7)

So, there are few aspects that correlate each other when it comes to the inlet gas temperature and flow rates to the AFM correspondence with Type HS, STD type and when AFM is not running.

6.4 Discussion on assumptions made

6.4.1 Temperature and moisture content of the raw materials going out from the coarse separator and cyclone system

As presented in the subchapter 5.7, lumped capacitance method was performed to validate the assumption that made to consider the raw material temperature that leaving coarse separator and the cyclone system equal to the gas temperature that leaving the cyclone system. i.e. $T_{RM,\ out} = T_{G,\ AFM\ out}$.

The actual residence time of a particle inside coarse separator and cyclone system typically lies between 0.5 s to 1 s with previous experiences. The residence time the particles require inside coarse separator and the cyclone systems to achieve the temperature same as the gas is calculated approximately as 0.3 s. Since actual residence time is greater than the theoretically calculated residence time, the assumption made can be justified as reasonable. Furthermore, the Biot number calculated was 0.00034. Since Biot number need to be less than 1 to validate the lumped capacitance method, the made assumption can be considered reasonable. See Table 5-10 for results of the lumped capacitance method calculation.

I addition, the thermal time constant, τ ($5.2*10^{-7}$ s) is a very low value, which implies the heating of the particles is very quicker. (i.e. lower the thermal time constant faster the heating of particles)

6.4.2 Temperature dependence of the heat capacity

Temperature dependence of the heat capacity was considered during the calculations to achieve more accurate answers during energy balances. Especially when heat availability calculation Type HS and STD type do have two levels of temperatures. (around 260 °C and around 180 °C). If the temperature dependence of the heat capacity was considered more accurate heat availability values can be obtained. The temperature dependency relationships of heat capacity values for individual gasses and raw materials are shown in Appendix H.

6.4.3 Moisture content and temperature of the inlet atmospheric air and raw materials coming into the raw meal department

The moisture content of the inlet raw materials and atmospheric air is a big uncertainty in the model. The moisture content of the air and raw materials can vary in a wide range due to the daily weather conditions. Since calculation was done in a winter period, the inlet atmospheric air temperature ($T_{A,\ in}$) was considered as 0 °C. The moisture content of the atmospheric air ($y_{H_2O,\ A,\ in}$) was calculated by obtaining maximum possible humid ratio at 0 °C which gave approximately 0.6% [14]. The inlet raw material temperature ($T_{RM,\ in}$) was measured, which varied around 0 °C.

FSA established at the raw material feeding belt to AFM is unable to measure the moisture content of the materials online. But the moisture content of individual raw materials (Dalen mine limestone, Verdal mine limestone, Bjorntvet quarry limestone, Serox etc.) is measured by plant physical laboratory monthly when they arrive at the plant. Analyzing those data revealed that it is hard to get an average value of the moisture contents of the samples. Since solid raw materials always expose to the environment during excavating, transportation, outside storage the water content in the raw materials affect directly by the environmental conditions. Typically, limestone moisture percentage ($x_{H_2O,\ RM,\ in}$) varies from 0.1% to 2% (mass percentage) where Serox moisture percentage varies from 2% to 8% (mass percentage). Furthermore, moisture content of the limestone from Bjorntvet quarry observed lower compared to moisture content of the limestone from Dalen and Verdal mines.

If the raw material moisture content is higher than the values taken into the calculation, more air is needed to be sent via AFM to fulfill the drying purpose. Then the heat availability at the bypass line possibly will reduce than the estimated value. See Figure 6-3 and Figure 6-5 for a graphical illustration of the heat required for the drying purpose (shown at the AFM). When Type HS is running, the heat required for drying is higher compared to STD type.

6.4.4 Heat loss estimation

According to the heat estimation shown in Table 5-8 the total estimated heat loss is less than 400 kW. Since surface temperatures were measured and areas were estimated by observing the general size of the equipment, possibly the actual heat loss can be slightly higher than the estimated value. 100 kW heat loss was assumed at ESP and BF since it was hard to take

temperature readings on the surfaces at the location. Average overall heat transfer co-efficient (U) was assumed as 10 $[W/m^2/K]$ which is inside typical overall heat transfer coefficient range for free gas convection with radiation [12]. Generally, when heat loses from insulated pipe surfaces to outside air, the radiation heat transfer does not make a big influence for the overall heat transfer [15].

6.4.5 Constant pressure inside the control volume

It has been assumed the pressure inside the control volume (P) is assumed as 101325 Pa even though there are pressure gradients in different locations to facilitate the gas flow generated by fans. The gauge pressures inside pipelines vary ±50 mbar. So, it is reasonable to assume a constant pressure for velocity conversions (real conditions to normal conditions) since a small pressure gradient does not make any difference (see equation (4.29)-(4.31)).

6.4.6 Composition of gas stream inside the control volume

The composition of the inlet gas stream does change slightly inside the control volume due to the false air induction, moisture vaporization from AFM drying, dust from raw materials. But it has been assumed that the gas composition is same as inlet gas composition so that the molecular weight of the gas stream would remain the same though-out the process. So, the density of the gas stream would remain same (see equation (4.40)) in order to simplify the calculation process.

6.5 Model validation

There are 3 extra equations that can be used to validate the results of the model. Oxygen balance at the AFM (4.15), energy balance at the gas separation point (4.21) and the energy balance at the AFM (4.27) was used to validate the model. Results from the model validation equations are shown in Table 6-4. A detail calculation for the model validation is shown at the end of Appendix D.

Table 6-4: Model validation results

Equation	Parameter	Type HS	STD type
Energy balance at the gas separation point (4.21)	$Q_{in,\ GS}$ (MW)	15.47	11.61
	$Q_{out,\ GS}$ (MW)	15.12	11.24
Energy balance at the AFM (4.27)	$Q_{input,\ AFM}$ (MW)	6.49	5.34
	$Q_{gain,\ AFM}$ (MW)	6.39	5.41
Oxygen balance at the AFM (4.15)	$y_{O_2, A, in}$	0.197	0.234

Energy balance at the gas separation point and at the AFM was calculated by dividing the equations into two sections to validate the model. At the gas separation point energy input to the junction ($Q_{in,\ GS}$) and energy output from the junction ($Q_{out,\ GS}$) were calculated separately. Energy output also includes the energy losses from the pipeline. For type HS energy input is 15. 47 MW and output is 15.12 MW. For STD type energy input and output are 11.61 MW and 11.24 MW respectively. There is a small heat difference in both scenarios. This is

probably due to the underestimated heat losses. Before gas stream enter to the AFM, gas stream goes via the burner (even though burner is not operating) where gas stream exposed to a larger volume suddenly. The surface of the burner is not insulated compared to the other areas. There is a several degrees temperature drop in the gas stream before entering to the AFM. So, there is a considerable heat loss at the point which is more than estimated. Furthermore, $T_{G,\ AFM\ in}$ temperature sensor is very close to the AFM and the temperature measurement probably affects by the false air entering to the AFM as well.

At the AFM, energy released by the hot gas stream and power input from the motor was calculated as heat input ($Q_{input,\ AFM}$). Heat gain by raw materials, false air including heat required to vaporize the moisture and heat losses were calculated as heat gain ($Q_{gain,\ AFM}$). For type HS energy input was calculated as 6.49 MW and energy gain and losses were calculated as 6.39 MW. For STD type energy input and gained energy were calculated as 5.34 MW and 5.41 MW respectively.

Considering energy inputs from fans and energy input from AFM motor directly affects to the gas stream is another probable explanation for energy deficiencies. A fraction of energy from fans and motor inputs do loose due to equipment wear, equipment noises, friction etc. Those losses have not been considered in the calculation. Furthermore, AFM motor power is directly used to rotate the AFM. When AFM is rotating the raw material particles inside the AFM do gain potential energy by raising them to a higher elevation and kinetic energy due to the rotation. But the energy conversion would not be 100% into the gas stream. And there is a huge noise made by the AFM due to the rotation and particle and ball colliding. Energy loss due to the noise also significant.

Another deficiency for the energy at the AFM would be uncertain data of the moisture content of the raw material as discussed in subchapter 6.4.3. It is unknown the exact moisture content of the raw materials at the moment where calculation was made (because the calculation was done using historical data). Average moisture values for the raw material mixtures were used for the calculation using pretested lab results when raw materials arrive at the plant. Moisture percentage of 1.02% for Type HS and 0.1% for STD type was used as raw material moisture content by weight. This is a big uncertainty in the calculation because the moisture value can vary in a big range due to the environment changes.

Using the oxygen balance equation at the AFM and finding the atmospheric oxygen mole fraction is a good indication to get a validation to the overall model. Since the atmospheric air oxygen mole fraction is known as 0.21 it is a good indication to compare the results as well.

Oxygen balance at the AFM gives oxygen mole fraction of the inlet atmospheric air as 0.197 and 0.234 for Type HS and STD type calculation respectively. Since the calculated atmospheric oxygen mole fraction values are closer to 0.21, the model can be considered as acceptable. Underestimation of heat losses during the energy balances at the AFM/BF and at gas mixing point is the probable explanation for not getting 0.21 as the exact value for atmospheric oxygen mole fraction. Energy balance equations have been used to calculate the mass flow rates hence volume flow rates directly affect the component balance.

6.6 Possibility of gas backflow via the bypass line

The possibility of gas stream backflow via the bypass gas line from the gas mixing point was investigated by analyzing temperature profiles for several data sets. Table 6-5 show the temperature data of the bypass gas stream ($T_{G,\ BP}$), temperature data of the gas stream coming after the main fan ($T_{G,\ AFM\ out}$) and temperature data of the combined gas stream ($T_{G,F,in}$),

bypass line gauge pressure (P_{BP}) and average valve openings for both Type HS and STD type. The temperature of the combined gas is always higher than the temperature of the gas stream that coming after the main fan ($T_{G,\,F,\,in} > T_{G,\ AFM\,out}$). If there is a backflow in the bypass line, thermodynamically the temperature of the combined gas stream should be lower than the temperature of the gas stream that coming after the main fan. So, it implies that there is no back-flow via the bypass line at any moment.

There is a pressure sensor inside the bypass line. When STD type is running it shows positive gauge pressure value which doesn`t imply that there is a backflow. Since the pressure sensor is close to the gas mixing point, there is a possibility of higher turbulence would affect the sensor measurements when STD type is running (Higher gas flow rate is sent via the AFM when STD type is running).

Table 6-5: Data for gas backflow analysis via the bypass line

Type/Date	$T_{G,\ BP}$ [°C]	$T_{G,\ AFM\ in}$ [°C]	$T_{G,\ AFM\ out}$ [°C]	$T_{G,\,F,\,in}$ [°C]	P_{BP} [mbar]	**Valve opening (%)**
STD (Data set 1)	183	182	60	95	0.63	58
STD (Data set 2)	186	182	63	100	0.21	56
STD (Data set 3)	190	188	65	100	0.53	67
HS (Data set 1)	262	257	63	129	0.07	39
HS (Data set 2)	266	254	54	125	-0.46	41
HS (Data set 3)	265	254	54	132	-0.31	31

6.7 Heat recovery possibility at the conditioning tower when AFM is not running

6.7.1 Drawbacks if water is not added at the conditioning tower when AFM is not running

The temperature of the gas stream would be approximately around 400 °C if the water is not added to the conditioning tower. This temperature is not an optimum temperature to achieve a good efficiency at the ESP just after the fan (see Figure 2-15 for ESP location). And the high temperature possibly can damage the ESP parts in the long run.

The average fan power usage of the fan after the conditioning tower (see Figure 2-15 for fan location) is around 900 kW when Type HS (temperature around 270 °C) is running. Fan power is directly proportional to the inlet gas temperature according to the equation (6.3) and (6.4). Which implies that there will be an increment of fan power when water is not added (when the AFM is not running) and that value is calculated as 430 kW. See Table 6-6 for fan power

calculation results when water is added to the gas stream and when water is not added to the gas stream.

So, the actual fan which is placed after the conditioning tower does not have enough power capacity to facilitate a gas flow with higher flow rate when the temperature is higher as 400 °C. This is another main reason, why water is added to the hot gas stream before sending it via raw meal department when AFM is running.

$$W_{el} = \frac{Cp_G T_{Fan,in} n_{flow\ rate}}{\eta_{fan}} \left(\left[\frac{P_{out}}{P_{in}} \right]^{R/Cp_G} - 1 \right) \tag{6.3}$$

$$W_{el} \propto T_{Fan,in} \tag{6.4}$$

If a new fan installed to facilitate high-temperature gas flow rates and plan to recover heat from the bypass gas stream at the raw meal department, the increment of the fan power (430 kW) is negligible compared to the available heat from the gas stream (approx. 30 MW, ref 0 °C). So, extra electricity that needs to run the fan if water is not added to the conditioning tower can be compensated by the available heat recovery.

Table 6-6: Fan power calculation with respect to the inlet gas temperature

Operating condition	**Average temperature before the fan (°C)**	**Average fan power (kW)**
Type HS (Water is added at the conditioning tower)	270	900
STD type (Water is added at the conditioning tower)	180	600
Not Running (Water is not added at the conditioning tower)	400	1330

6.7.2 Best possibility to recover heat when AFM is not running

So, when AFM is not running the best option to recover the heat is to place a couple of heat exchangers in series (for LP steam and hot water production) before the ESP instead of passing the gas via the conditioning tower. Heat recovery using the available heat before ESP when AFM is not running is shown in a Sankey diagram (see Figure 6-14). The average yearly available heat is calculated as 52 TJ per year for LP steam generation and 16 TJ per year for hot water generation (see subchapter 5.3 for calculation).

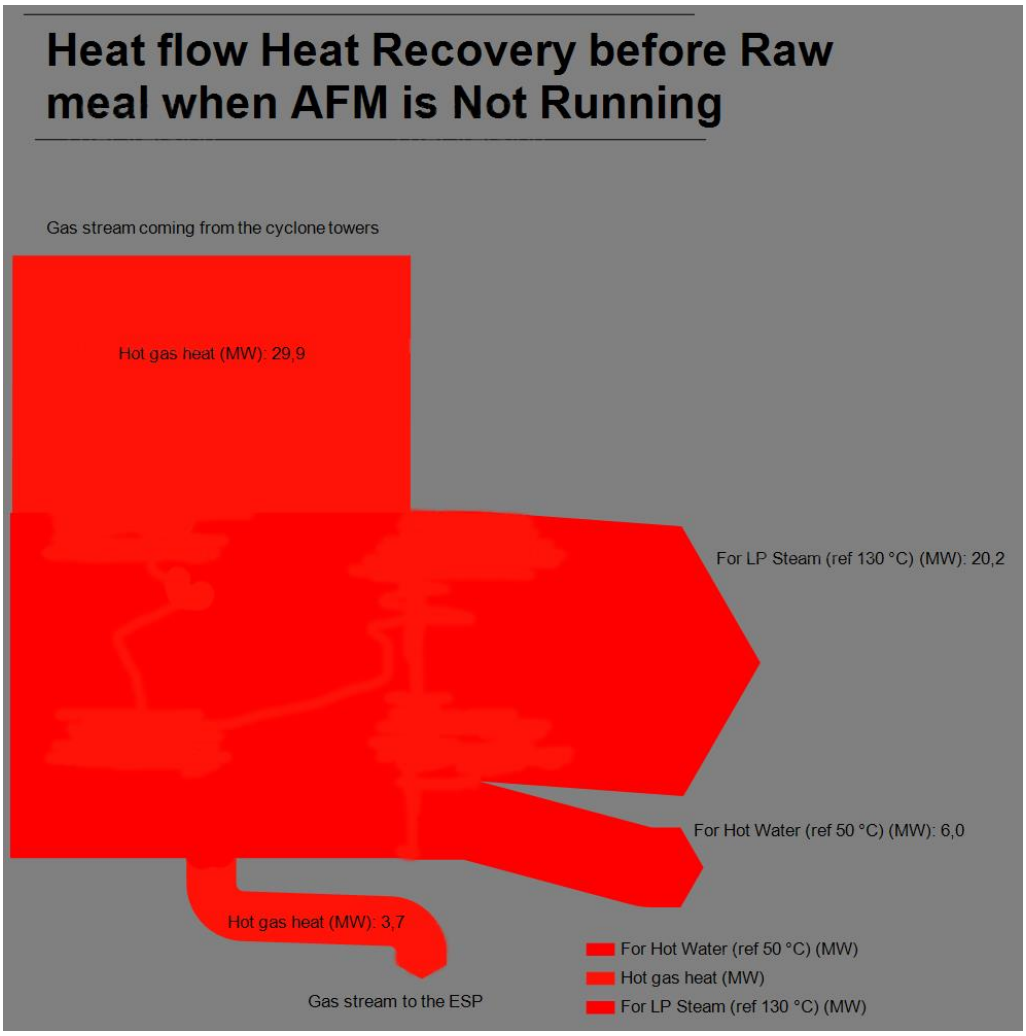

Figure 6-14: Sankey diagram for the heat flows with possible heat recovery before the raw meal department when AFM is not running

6.8 False air coming into the raw meal department

False air coming into the main gas streams in the raw meal department is significant according to the estimations. It has been estimated 40% to 50 % volume of air in the outlet gas stream leaving the raw meal department (stream number 6 in Figure 4-2) is the false air that enters to the raw meal department (see Table 6-7). Key places that false air coming into the system are at the AFM and at the ESP and the BF. As per the results in Table 6-7 most of the false air is coming into the system coming from the raw material feeding inlet at the AFM. Only about 10% to 15% of false air coming into the system via ESP and the BF. False air only entering via ESP and the BF to the gas stream when AFM is not running.

Furthermore, it is hard to find a proper relationship of the false air coming into the system versus process type inside the raw meal department. But the amount of false air coming into the system at AFM is important when it's come to the heat recovery at the bypass gas stream. When false air entering the AFM, the temperature is very low (between 0 °C and 25 °C). So, there is a sensible heat transfer from the hot gas stream that is sent via the AFM to heat up the false air. Since one of the main purpose of sending hot gas via AFM is to dry the raw materials,

if the false air coming via the raw material feed opening at AFM can be minimized then more air can be bypassed. So, more heat recovery can be achievable at the bypass gas stream.

Table 6-7: False air coming into the raw meal department

Process Type	False air at AFM (Vol %)	False air at ESP and BF (Vol %)	Total false air (Vol %)
Type HS	28 %	15 %	43 %
STD type	36 %	8 %	44 %
AFM not running	0 %	9 %	9 %

6.9 End temperature selection for heat recovery

For heat recovery, the suggested way is to use a series of heat exchangers to generate LP steam and hot water. Figure 6-15 shows a suggested heat exchanger system to generate LP steam and hot water using the available heat near the bypass gas stream at the raw meal department. The similar arrangement can be used at the conditioning tower if heat recovery is planned at the place when AFM is not running. LP steam is suggested to generate until hot gas become 130 °C (i.e. end temperature of 130 °C) and hot water is suggested to generate till hot gas stream become 50 °C (i.e. end temperature of 50 °C) from 130 °C. LP steam is expected at around 140 °C with 360 kPa pressure which is a typical value for industrial LP steam and hot water is expected at approximately 60 °C according to the requirement which is a typical hot water temperature that required to heating purposes and domestic hot water usage [10]. Furthermore, output temperatures of the LP steam and hot water are decided in order to maintain a minimum 10 °C temperature gradient for the driving force to heat transfer ($\Delta T_{min} > 10\,°C$). The temperature of the generated LP steam and hot water can be changed slightly due to process conditions. Inlet water temperature could be varying between 0 °C to 25 °C due to climate changes. Approximately calculated amounts of LP steam and hot water for different process conditions are shown in Table 6-1.

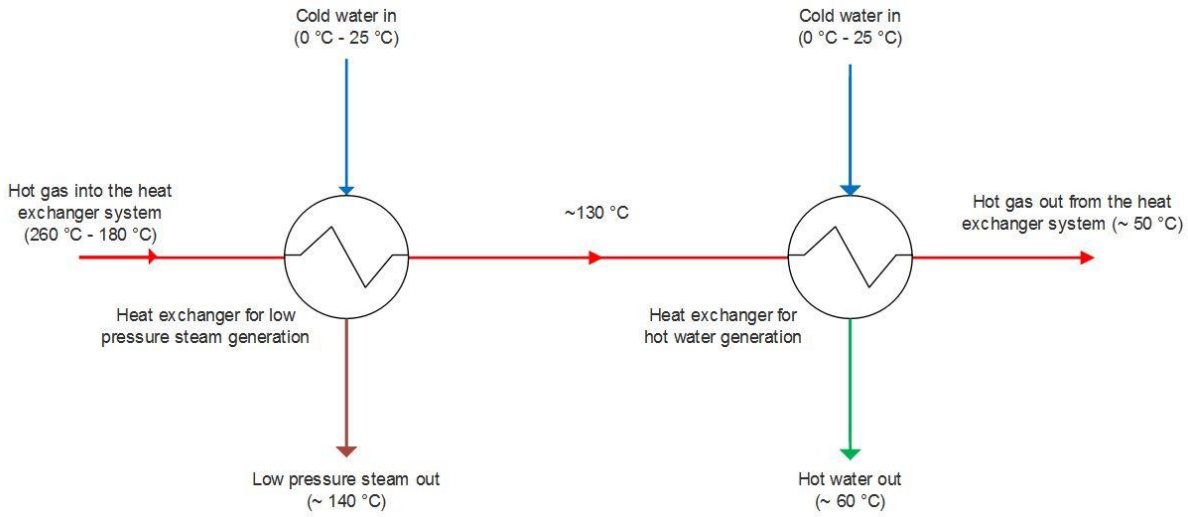

Figure 6-15: Suggested heat exchanger system for LP steam generation and hot water generation

6.10 Possible issues with heat recovery

As mentioned in subchapter 6.2.3 there is a fraction of dust mass accumulated in the hot gas inside the bypass line and before conditioning tower as well. Probably in most industries uses shell and tube heat exchangers to recover heat from the gas streams. In that case, gas streams must be sent via the tubes to minimize the deposition of dust inside the heat exchanger. If gas stream is sent via the shell side, due to the baffles and other obstacles there is a high possibility to deposit more dust inside. Even if gas is sent via the tubes dust possibly can be accumulated but at a slower rate. This may lead to fouling and less heat recovery. And further deposition may lead to blockage of the tubes. So, proper maintenance procedures need to be followed to remove the accumulated dust inside the tubes.

Moisture inside the gas stream is an important parameter when the gas stream is used to heat recovery. Moisture in the gas stream will condense inside the heat exchanger which is designated to produce hot water since hot gas temperature reduces from 130 °C to 50 °C during the heat transfer. Possibly this condensed moisture will make a pulp with accumulated dust inside the tube of the heat exchanger which will lead to hard maintenance processes, gas blockages etc. So, additional precautions need to be taken to remove the excess moisture that condensed.

7 Conclusion and Recommendations

The main aim of this study was to find out the available heat of the exhaust gas that is bypassed through the raw meal department to recover the available heat. With an exhaust gas temperature coming into the raw meal department in the order of 180-260 °C, the heat can be utilized to generate low-pressure stream (~130 °C) and hot water (~50 °C). The available heat varies from 1.5 MW to 4.2 MW for LP steam (0.5 kg/s - 1.5 kg/s) and 2.2 MW to 5.8 MW for hot water generation (8 kg/s - 23 kg/s) at the bypass line, depending on the operating conditions at the raw meal department. This means that a significant amount of waste heat is available and can be utilized for energy utilizing purposes.

The available heat is low when STD type is running compared to other process conditions. Approximately a heat of 20 MW for LP steam and 6 MW for hot water generation is available at the conditioning tower before the raw meal department when AFM is not running. The average yearly available heat is approximately 50 TJ per year at the conditioning tower when AFM is not running. So, it is recommended to extract available heat via bypass line when Type HS and STD type is running and extract heat by bypassing gas stream from the conditioning tower when AFM is not running.

A network of heat exchangers is suggested to recover heat. The heat loss from the system and power inputs from fans and motors are negligible compared to the available heat. It has been found that there is no gas recycling via the bypass line. Furthermore, the total false air coming into the system from different locations has been estimated as 40-50% of total air going out from the raw meal department.

As for suggestions for further work, it is better to establish a pilot heat exchanger system by extracting a fraction of the bypass gas stream to identify the real process conditions and obstacles further. A cost analysis needs to be done to estimate the capital cost required for the equipment that needs for the heat recovery along with an operating cost analysis and payback calculation.

8 References

[1] "Norcem Brevik," [Online]. Available: http://www.norcem.no/en/brevik. [Accessed 7 January 2017].

[2] M. Hepberger, "ORC Waste Heat Recovery system using kiln exit and cooler vent air," in *VDZ Jahrestagung*, Düsseldorf, 2012.

[3] Yana Gorbatenko, Alexander Sharabaroff, Bruce Hedman, Jigar Shah, "Waste Heat Recovery," Institute for Industrial Productivity, International Finance Corporation, [Online]. Available: http://www.iipnetwork.org/62730%20WRH_Report.pdf2. [Accessed 2 May 2017].

[4] Ernst Worrell, Christina Galitsky, "Energy Efficiency Improvement Opportunities for Cement Making," Berkeley, California, January 2004.

[5] S K Gupta, S K Kaul, "Waste heat recovery power plants in cement," Holtec Consulting Private Ltd, Gurgaon, India, [Online]. Available: http://www.holtecnet.com/holtecdocs/TechnicalPapers/p_2011_6.pdf. [Accessed 5 March 2017].

[6] S. Nivethidha Priyadarshini, D. B. Sivakumar, "Waste Heat Recovery in Cement plant," *nternational Journal of Engineering Research & Technology (IJERT),* vol. 3, no. 5, pp. 814-818, 2014.

[7] P. B.V., "PANalytical," Spectris plc, 2017. [Online]. Available: http://www.panalytical.com/CNA-PentosCement/Features.htm. [Accessed 11 January 2017].

[8] T. I. Solutions, "Aerofall mill as autogenus and semi-autogenous mill," ThyssenKrupp Industrial Solutions (USA), 2014. [Online]. Available: http://www.polysiususa.com/minerals/grinding_plants/Dry_grinding_plants/aerofall_mill.html. [Accessed 11 January 2017].

[9] Ron Zevenhoven, Pia Kilpinen, "Particulates," in *Control of pollutants*, Finland, 2004, pp. 5-15.

[10] "Properties of Saturated Steam," Engineering ToolBox, [Online]. Available: http://www.engineeringtoolbox.com/saturated-steam-properties-d_101.html. [Accessed 12 April 2017].

[11] "Water - Thermodynamic Properties," Engineering ToolBox, [Online]. Available: http://www.engineeringtoolbox.com/water-thermal-properties-d_162.html. [Accessed 12 April 2017].

[12] "Typical Overall Heat-Transfer Coefficients," [Online]. Available: http://www.engineeringtoolbox.com/overall-heat-transfer-coefficient-d_434.html. [Accessed 15 February 2017].

[13] P. Nag, "Heat and mass transfer," in *Transient heat conduction*, New Delhi, Tata McGraw-Hill, 2007, pp. 179-183.

[14] "Humidity Ratio of Air, Humidity Ratio by Vapor Partial Pressure," Engineering ToolBox, [Online]. Available: http://www.engineeringtoolbox.com/humidity-ratio-air-d_686.html. [Accessed 15 February 2017].

[15] Zoran K. Morvay, Dusan D., "Applied Industrial Energy and Environmental Management," [Online]. Available: http://www.wiley.com/legacy/wileychi/morvayindustrial/supp/toolbox10.pdf. [Accessed 2 May 2017].

[16] I. Chemstations, "CHEMCAD 6.1.3," Houston, Texas , 2017.

Appendices

Appendix A: Thesis summary page

Appendix B: Calculation data sheet for Type HS

Appendix C: Inlet gas dust concentration estimation

Appendix D: Detail systematic calculation for Type HS and model validation

Appendix E: Possible LP steam and hot water generation calculation

Appendix F: Detail calculation for inlet gas moisture fraction estimation for Type HS

Appendix G: Detail calculation for lumped capacitance method

Appendix H: Heat capacity relationships

Appendix A: Thesis summary page

University College of Southeast Norway

Faculty of Technology, Natural Sciences and Maritime Sciences, Campus Porsgrunn

FMH606 Master's Thesis

Title: Waste heat availability in a raw meal production facility

HSN supervisor: Professor Lars-André Tokheim

External partner: Norcem (Ida Husum, Manager of Process and Environment)

Task background:

At the Norcem cement plant in Brevik, in the raw meal department, different types of limestone and additives are mixed and ground into a fine powder called raw meal. The raw meal is used downstream in the process as kiln feed, for production of clinker, which in turn is used further downstream in the process as feed to the cement mills.

In the raw meal department, a hot exhaust gas coming from the kiln is used to dry the raw materials and also to control the raw meal production rate. Part of the exhaust gas goes through a ball mill ("aerofall mill"), and the rest is bypassing the ball mill. Downstream of the ball mill, the partly ground raw meal is separated from the gas and is then passed on to a roller press for further grinding. The exhaust gas is mixed with the bypass gas, dedusted in a filter system and finally released to the surroundings via a stack. Depending on what type of raw meal is produced, the fraction of the gas going through the mill can vary quite a lot.

The gas bypassing the ball mill contains sensible heat that may be utilized for other purposes, and Norcem is considering the installation of a heat exchanger in order to utilize this waste heat in another process. To be able to evaluate the waste heat availability, data on variation in gas flow rate, temperature and other characterstics, in different parts of the system, are required. Some data are partly available, after having run separate measurement campaigns at the plant, but a mass and energy balance is required to make full use of these data. Additional measurements may be made if necessary, equipment (pitot tubes, thermocouples, and possibly a portable gas analyzer) will then be made available.

Task description:

The task should include the following sub-tasks:

- Problem description and goal definition
- Process system description
- Development of a mass and energy balance
- Analysis of data collected in lab test campaigns
- If necessary, additional measurements of gas flow and characterstics
- Application of collected data in the mass and energy balance
- Quantification of, and conclusion about, the waste heat availability in the raw meal department based on the measurement data and the mass and energy balance

Address: Kjølnes ring 56, NO-3918 Porsgrunn, Norway. **Phone:** 35 57 50 00. **Fax:** 35 55 75 47.

Student category: PT and EET

Practical arrangements:

Some meetings at Norcem Brevik are required to plan the work and discuss the progress. Also, if relevant, the student may carry out or take part in the execution of measurements in the raw meal department at Norcem Brevik. Apart from this, the work will mainly be carried out at USN.

Signatures:

Student (date and signature): 26/01/2017

Supervisor (date and signature): Lars Arbo Tokheim, 26/1-17

Appendix B: Calculation data sheet for Type HS

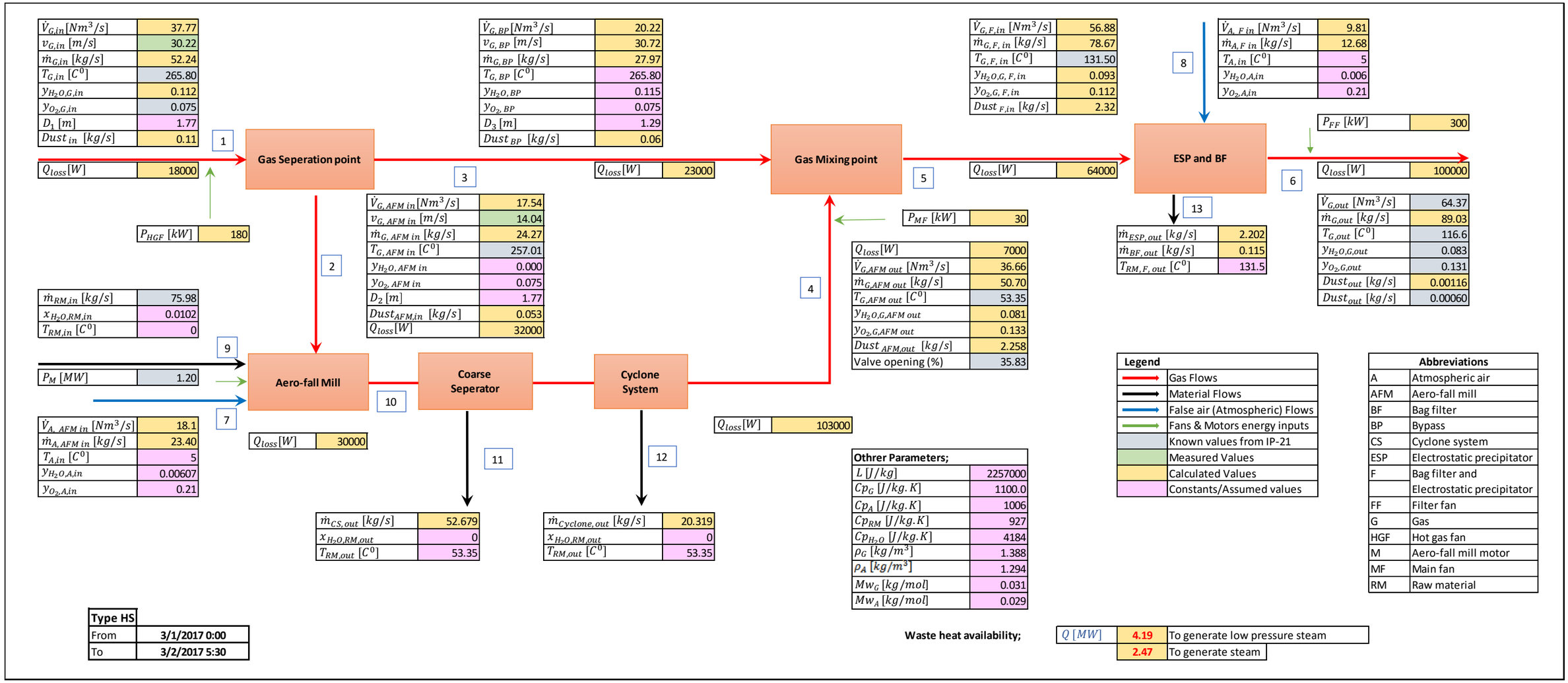

$\dot{V}_{G,in}[Nm^3/s]$	37.77
$v_{G,in}\ [m/s]$	30.22
$\dot{m}_{G,in}\ [kg/s]$	52.24
$T_{G,in}\ [C^0]$	265.80
$y_{H_2O,G,in}$	0.112
$y_{O_2,G,in}$	0.075
$D_1\ [m]$	1.77
$Dust_{in}\ [kg/s]$	0.11

$Q_{loss}[W]$	18000

$P_{HGF}\ [kW]$	180

$\dot{m}_{RM,in}\ [kg/s]$	75.98
$x_{H_2O,RM,in}$	0.0102
$T_{RM,in}\ [C^0]$	0

$P_M\ [MW]$	1.20

$\dot{V}_{A,\ AFM\ in}\ [Nm^3/s]$	18.1
$\dot{m}_{A,\ AFM\ in}\ [kg/s]$	23.40
$T_{A,in}\ [C^0]$	5
$y_{H_2O,A,in}$	0.00607
$y_{O_2,A,in}$	0.21

$Q_{loss}[W]$	30000

$\dot{V}_{G,BP}[Nm^3/s]$	20.22
$v_{G,BP}\ [m/s]$	30.72
$\dot{m}_{G,BP}\ [kg/s]$	27.97
$T_{G,BP}\ [C^0]$	265.80
$y_{H_2O,BP}$	0.115
$y_{O_2,BP}$	0.075
$D_3\ [m]$	1.29
$Dust_{BP}\ [kg/s]$	0.06

$Q_{loss}[W]$	23000

$\dot{V}_{G,AFM\ in}[Nm^3/s]$	17.54
$v_{G,AFM\ in}\ [m/s]$	14.04
$\dot{m}_{G,AFM\ in}\ [kg/s]$	24.27
$T_{G,AFM\ in}\ [C^0]$	257.01
$y_{H_2O,AFM\ in}$	0.000
$y_{O_2,AFM\ in}$	0.075
$D_2\ [m]$	1.77
$Dust_{AFM,in}\ [kg/s]$	0.053
$Q_{loss}[W]$	32000

$\dot{m}_{CS,out}\ [kg/s]$	52.679
$x_{H_2O,RM,out}$	0
$T_{RM,out}\ [C^0]$	53.35

$\dot{m}_{Cyclone,out}\ [kg/s]$	20.319
$x_{H_2O,RM,out}$	0
$T_{RM,out}\ [C^0]$	53.35

$Q_{loss}[W]$	103000

$P_{MF}\ [kW]$	30

$Q_{loss}[W]$	7000
$\dot{V}_{G,AFM\ out}\ [Nm^3/s]$	36.66
$\dot{m}_{G,AFM\ out}\ [kg/s]$	50.70
$T_{G,AFM\ out}\ [C^0]$	53.35
$y_{H_2O,G,AFM\ out}$	0.081
$y_{O_2,G,AFM\ out}$	0.133
$Dust_{AFM,out}\ [kg/s]$	2.258
Valve opening (%)	35.83

$\dot{V}_{G,F,in}\ [Nm^3/s]$	56.88
$\dot{m}_{G,F,in}\ [kg/s]$	78.67
$T_{G,F,in}\ [C^0]$	131.50
$y_{H_2O,G,F,in}$	0.093
$y_{O_2,G,F,in}$	0.112
$Dust_{F,in}\ [kg/s]$	2.32

$Q_{loss}[W]$	64000

$\dot{V}_{A,\ F\ in}\ [Nm^3/s]$	9.81
$\dot{m}_{A,F\ in}\ [kg/s]$	12.68
$T_{A,in}\ [C^0]$	5
$y_{H_2O,A,in}$	0.006
$y_{O_2,A,in}$	0.21

$P_{FF}\ [kW]$	300

$Q_{loss}[W]$	100000

$\dot{V}_{G,out}\ [Nm^3/s]$	64.37
$\dot{m}_{G,out}\ [kg/s]$	89.03
$T_{G,out}\ [C^0]$	116.6
$y_{H_2O,G,out}$	0.083
$y_{O_2,G,out}$	0.131
$Dust_{out}\ [kg/s]$	0.00116
$Dust_{out}\ [kg/s]$	0.00060

$\dot{m}_{ESP,out}\ [kg/s]$	2.202
$\dot{m}_{BF,out}\ [kg/s]$	0.115
$T_{RM,F,out}\ [C^0]$	131.5

Othrer Parameters;	
$L\ [J/kg]$	2257000
$Cp_G\ [J/kg.K]$	1100.0
$Cp_A\ [J/kg.K]$	1006
$Cp_{RM}\ [J/kg.K]$	927
$Cp_{H_2O}\ [J/kg.K]$	4184
$\rho_G\ [kg/m^3]$	1.388
$\rho_A\ [kg/m^3]$	1.294
$Mw_G\ [kg/mol]$	0.031
$Mw_A\ [kg/mol]$	0.029

From	3/1/2017 0:00
To	3/2/2017 5:30

Appendix C: Inlet gas dust concentration estimation

- Dust mass flow rate coming out from the cyclone tower estimation using equation (5.8);

$$Dust_{tower,\ out} = \dot{m}_{RM,\ tower,\ in} * \left(1 - \eta_{Cyclone}\right)$$

$$Dust_{tower,\ out} = 115 * (1 - 0.9)\ t/h$$

$$Dust_{tower,\ out} = 11.5\ t/h$$

- Dust mass flow rate coming out from the ESP (no.3) estimation using equation (5.9);

$$Dust_{ESP3,\ out} = Dust_{tower,\ out} * (1 - \eta_{ESP})$$

$$Dust_{ESP3,\ out} = 11.5 * (1 - 0.95)\ t/h$$

$$Dust_{ESP3,\ out} = 0.575\ t/h$$

- Dust concentration in the hot gas stream estimation using equation (5.10);

$$C_{Dust,in} = \frac{Dust_{ESP3,\ out} * 10^6}{\dot{V}_{G,\ in}}$$

$$C_{Dust,in} = \frac{0.575 * 10^6}{190000} g/Nm^3$$

$$C_{Dust,in} = 3\ g/Nm^3$$

Appendix D: Detail systematic calculation for Type HS and model validation

- Gas stream molecular weight;

Component	Volume Percentage	Mw (kg/mol)	Volume Percentage*Mw	
N_2	61%	0.028	0.0171976	
CO_2	22%	0.044	0.0097768	
O_2	7%	0.032	0.0022496	
H_2O	10%	0.018	0.0018	
SO_2	0%	0.064	0.00000016	
Dust/limestone	0%	0.1	0.0000672	
Mw of gas stream (M_{wG})			**0.0311**	kg/mol

- $\dot{V}_{G,\ in}$ using the measured $v_{G,\ in}$ value estimation using the equation (4.29);

$$\dot{V}_{G,\ in} = \frac{\pi}{4} * {D_1}^2 * v_{G,\ in} * \frac{T_N * P}{T_{G,\ in} * P_N}$$

$$\dot{V}_{G,\ in} = \frac{\pi}{4} * 1.77^2 * 30.22 * \frac{273.15 * 101325}{(265.8 + 273.15) * 101325}\ Nm^3/s$$

$$\dot{V}_{G,\ in} = 37.7\ Nm^3/s$$

- $\dot{m}_{G,\ in}$ calculation estimation using the equation (4.32);

$$\dot{m}_{G,\ in} = \rho_G * \dot{V}_{G,\ in}$$

$$\dot{m}_{G,\ in} = 1.388 * 37.7\ kg/s$$

$$\dot{m}_{G,\ in} = 52.3\ kg/s$$

- Dust mass flow rate calculation at gas separation point estimation using the equations (4.2)-(4.4)[2];

$$Dust_{\ in} = \frac{\dot{V}_{G,\ in} * C_{Dust,in}}{1000}$$

$$Dust_{\ in} = \frac{37.7 * 3}{1000}\ kg/s$$

[2] $\dot{m}_{G,\ BP}$ Initially assumed as zero (negligible value) for mass and energy balance calculations at ESP and BF

$$Dust_{in} = 0.113\ kg/s$$

$$Dust_{BP} = Dust_{in} * \frac{\dot{m}_{G,\ BP}}{\dot{m}_{G,\ in}}$$

$$Dust_{BP} = 0.113 * \frac{27.97}{52.3}\ kg/s$$

$$Dust_{BP} = 0.06\ kg/s$$

$$Dust_{AFM,\ in} = Dust_{in} - Dust_{BP}$$

$$Dust_{AFM,\ in} = 0.113 - 0.06\ kg/s$$

$$Dust_{AFM,\ in} = 0.053\ kg/s$$

- Raw material mass flow rates calculation at coarse separator and cyclone system using the equation (4.6) and (4.7);

$$\dot{m}_{CS,\ out} = [\dot{m}_{RM,\ in} * (1 - x_{H_2O,\ RM,\ in}) + Dust_{AFM,\ in}] * \eta_{CS}$$

$$\dot{m}_{CS,\ out} = [75.98 * (1 - 0.0102) + 0.053] * 0.7\ kg/s$$

$$\dot{m}_{CS,\ out} = 52.68\ kg/s$$

$$\dot{m}_{Cyclone,\ out} = [\dot{m}_{RM,\ in} * (1 - x_{H_2O,\ RM,\ in}) + Dust_{AFM,\ in} - \dot{m}_{CS,\ out}] * \eta_{Cyclone}$$

$$\dot{m}_{Cyclone,\ out} = [75.98 * (1 - 0.0102) + 0.053 - 52.68] * 0.9\ kg/s$$

$$\dot{m}_{Cyclone,\ out} = 20.32\ kg/s$$

- Dust mass flow rates calculation at gas mixing point using the equation (4.8) and (4.10);

$$Dust_{AFM,\ out} = [\dot{m}_{RM,\ in} * (1 - x_{H_2O,\ RM,\ in}) + Dust_{AFM,\ in} - \dot{m}_{CS,\ out} - \dot{m}_{Cyclone,\ out}]$$

$$Dust_{AFM,\ out} = [75.98 * (1 - 0.0102) + 0.053 - 52.68 - 20.32]\ kg/s$$

$$Dust_{AFM,\ out} = 2.258\ kg/s$$

$$Dust_{F,\ in} = Dust_{BP} + Dust_{AFM,\ out}$$

$$Dust_{F,\ in} = (0.06 + 2.258)\ kg/s$$

$$Dust_{F,\ in} = 2.318\ kg/s$$

- Raw material and dust mass flow rates calculation at ESP and BF using the equations (4.12)-(4.14) ;

$$\dot{m}_{ESP,\ out} = Dust_{\ F,in} * \eta_{ESP}$$
$$\dot{m}_{ESP,\ out} = 2.318 * 0.95\ kg/s$$
$$\dot{m}_{ESP,\ out} = 2.202\ \text{kg/s}$$

$$\dot{m}_{BF,\ out} = (Dust_{\ F,in} - \dot{m}_{ESP,\ out}) * \eta_{BF}$$
$$\dot{m}_{BF,\ out} = (2.318 - 2.202) * 0.99\ kg/s$$
$$\dot{m}_{BF,\ out} = 0.115\ kg/s$$

$$Dust_{out}\ = (Dust_{\ F,in} - \dot{m}_{ESP,\ out} - \dot{m}_{BF,\ out})$$
$$Dust_{out}\ = (2.318 - 2.202 - 0.115)\ kg/s$$
$$Dust_{out}\ = 0.001\ kg/s$$

- Density parameter calculations using the equations (4.40)-(4.42);

$$\rho_G = \frac{P_N * M_{wG}}{R * T_N}$$
$$\rho_G = \frac{101325 * 0.0311}{8.314 * 273.15}\ kg/m^3$$
$$\rho_G = 1.388\ kg/m^3$$

$$\rho_A = \frac{P_N * M_{wA}}{R * T_N}$$
$$\rho_A = \frac{101325 * 0.029}{8.314 * 273.15}\ kg/m^3$$
$$\rho_A = 1.294\ kg/m^3$$

$$\rho_{H_2O} = \frac{P_N * M_{wH_2O}}{R * T_N}$$
$$\rho_{H_2O} = \frac{101325 * 0.018}{8.314 * 273.15}\ kg/m^3$$
$$\rho_{H_2O} = 0.803\ kg/m^3$$

- Mass flow rate calculation at the outlet (after the ESP and BF) - ($\dot{m}_{G,\ out}$) using the equation (4.39);

$$\dot{m}_{G,\ out} = \rho_G * \dot{V}_{G,\ out}$$
$$\dot{m}_{G,\ out} = 1.388 * 64.37\ kg/s$$
$$\dot{m}_{G,\ out} = 89\ kg/s$$

- Mass flow rate calculation at ESP and BF using the equations (4.28) and (4.11);

  Energy balance equation;

$$\dot{m}_{G,F,in} * Cp_G * T_{G,\ F,\ in} + \dot{m}_{A,\ F\ in} * Cp_A * T_{A,\ in} + P_{FF} = \dot{m}_{G,\ out} * Cp_G * T_{G,\ out} + (\dot{m}_{ESP,\ out} + \dot{m}_{BF,\ out}) * Cp_{RM} * T_{RM,\ F,\ out} + Q_{loss}$$

$$\dot{m}_{G,F,in} * 1057 * 131.5 + \dot{m}_{A,\ F\ in} * 1006 * 5 + 300 * 1000 = 89.03 * 1052 * 116.6 + (2.202 + 0.115) * 927 * 131.5 + 100000$$

  Mass balance equation;

$$\dot{m}_{G,\ out} + \dot{m}_{ESP,\ out} + \dot{m}_{BF,\ out} = \dot{m}_{G,F,in} + \dot{m}_{A,\ F\ in}$$
$$89.03 + 2.202 + 0.115 = \dot{m}_{G,F,in} + \dot{m}_{A,\ F\ in}$$

  Solving above two equations gives;

$$\dot{m}_{G,F,in} = 78.67\ kg/s$$
$$\dot{m}_{A,\ F\ in} = 12.68\ kg/s$$

- Volume flow rate calculation at ESP and BF using the equations (4.37) and (4.38);

$$\dot{m}_{A,\ F\ in} = \rho_A * \dot{V}_{A,\ F\ in}$$
$$12.68 = 1.294 * \dot{V}_{A,\ F\ in}$$
$$\dot{V}_{A,\ F\ in} = 9.8\ Nm^3/s$$

$$\dot{m}_{G,\ F\ in} = \rho_G * \dot{V}_{G,\ F\ in}$$
$$78.67 = 1.388 * \dot{V}_{G,\ F\ in}$$
$$\dot{V}_{G,\ F\ in} = 56.8\ Nm^3/s$$

- Moisture and oxygen calculation at ESP and BF using the equations (4.19) and (4.17);

$$\dot{V}_{G,\ out} * y_{H_2O,G,\ out} = \dot{V}_{G,\ F,in} * y_{H_2O,G,F,in} + \dot{V}_{A,\ F\ in} * y_{H_2O,A,\ in}$$

$$64.37 * 0.083 = 56.8 * y_{H_2O,\,G,\,F,\,in} + 9.8 * 0.006$$

$$y_{H_2O,\,G,\,F,\,in} = 0.093$$

$$\dot{V}_{G,\ out} * y_{O_2,\,G,\ out} = \dot{V}_{G,\ F,\,in} * y_{O_2,\,G,\,F,\ in} + \dot{V}_{A,\ F\,in} * y_{O_2,\,A,\,in}$$

$$64.37 * 0.131 = 56.8 * y_{O_2,\,G,\,F,\ in} + 9.8 * 0.21$$

$$y_{O_2,\,G,\,F,\ in} = 0.112$$

- Mass flow rate calculation at gas mixing point using the equations (4.22) and (4.9);

  Energy balance equation;

$$\dot{m}_{G,\,F,in} * Cp_G * T_{G,\ F,\ in} = \dot{m}_{G,\ BP} * Cp_G * \dot{T}_{G,\ BP} + P_{MF} + m_{G,\ AFM\,out} * Cp_G * T_{G,\ AFM\,out} - Q_{loss}$$

$$78.67 * 1057 * 131.5 = \dot{m}_{G,\ BP} * 1102 * 265.8 + 30000 + \dot{m}_{G,\ AFM\,out} * 1029 * 53.35 - (64000 + 7000)$$

  Mass balance equation;

$$\dot{m}_{G,\,F,in} = \dot{m}_{G,\ BP} + \dot{m}_{G,\ AFM\,out}$$

$$78.67 = \dot{m}_{G,\ BP} + \dot{m}_{G,\ AFM\,out}$$

  Solving above two equations gives;

$$\dot{m}_{G,\ BP} = 27.97\ kg/s$$

$$\dot{m}_{G,\ AFM\,out} = 50.7\ kg/s$$

- Volume flow rate and gas velocity calculation at bypass gas stream and for the gas stream coming out from the cyclone system using the equations (4.33), (4.30) and (4.36);

$$\dot{m}_{G,\ BP} = \rho_G * \dot{V}_{G,\ BP}$$

$$27.97 = 1.388 * \dot{V}_{G,\ BP}$$

$$\dot{V}_{G,\ BP} = 20.2\ Nm^3/s$$

$$\dot{V}_{G,\ BP} = \frac{\pi}{4} * {D_3}^2 * v_{G,\ BP} * \frac{T_N * P}{T_{G,\ in} * P_N}$$

$$20.2 = \frac{\pi}{4} * 1.29^2 * v_{G,\ BP} * \frac{273.15 * 101325}{(265.8 + 273.15) * 101325}$$

$$v_{G,\ BP} = 30.7\ m/s$$

$$\dot{m}_{G,\ AFM\ out} = \rho_G * \dot{V}_{G,\ AFM\ out}$$

$$50.7 = 1.388 * \dot{V}_{G,\ AFM\ out}$$

$$\dot{V}_{G,\ AFM\ out} = 36.6\ Nm^3/s$$

- Oxygen and moisture calculation for the gas stream coming out from the cyclone system using the equations (4.16) and (4.18);

$$\dot{V}_{G,\ F,in} * y_{O_2,G,F,\ in} = \dot{V}_{G,\ BP} * y_{O_2,\ BP} + \dot{V}_{G,\ AFM\ out} * y_{O_2,\ G,AFM\ out}$$

$$56.8 * 0.112 = 20.2 * 0.075 + 36.6 * y_{O_2,\ G,AFM\ out}$$

$$y_{O_2,\ G,AFM\ out} = 0.133$$

$$\dot{V}_{G,\ F,in} * y_{H_2O,G,\ F,\ in} = \dot{V}_{G,\ BP} * y_{H_2O,\ BP} + \dot{V}_{G,\ AFM\ out} * y_{H_2O,G,AFM\ out}$$

$$56.8 * 0.093 = 20.2 * 0.112 + 36.6 * y_{H_2O,G,AFM\ out}$$

$$y_{H_2O,G,AFM\ out} = 0.083$$

- Mass and volume flow rate and gas velocity calculation at gas separating point using the equations (4.1), (4.34) and (4.31);

$$\dot{m}_{G,\ in} = \dot{m}_{G,\ BP} + \dot{m}_{G,\ AFM\ in}$$

$$52.3 = 27.97 + \dot{m}_{G,\ AFM\ in}$$

$$\dot{m}_{G,\ AFM\ in} = 24.3\ kg/s$$

$$\dot{m}_{G,\ AFM\ in} = \rho_G * \dot{V}_{G,\ AFM\ in}$$

$$24.3 = 1.388 * \dot{V}_{G,\ AFM\ in}$$

$$\dot{V}_{G,\ AFM\ in} = 17.5\ Nm^3/s$$

$$17.5 = \frac{\pi}{4} * 1.77^2 * v_{G,\ AFM\ in} * \frac{273.15 * 101325}{(265.8 + 273.15) * 101325}$$

$$v_{G,\ AFM\ in} = 14.03\ m/s$$

- Mass and volume flow rate calculation at gas AFM using the equations (4.5) and (4.35);

$$\dot{m}_{G,\ AFM\ out} = \dot{m}_{G,\ AFM\ in} + \dot{m}_{A,\ AFM\ in} + \dot{m}_{RM,\ in} * x_{H_2O,RM,\ in} + Dust_{\ AFM,out}$$

$$50.7 = 24.3 + \dot{m}_{A,\ AFM\ in} + 75.98 * 0.0102 + 2.258$$

$$\dot{m}_{A,\ AFM\ in} = 23.4\ kg/s$$

$$\dot{m}_{A,\ AFM\ in} = \rho_A * \dot{V}_{A,\ AFM\ in}$$

$$23.4 = 1.294 * \dot{V}_{A,\ AFM\ in}$$

$$\dot{V}_{A,\ AFM\ in} = 18.1\ Nm^3/s$$

- Inlet gas moisture calculation ($y_{H_2O,G,in}$) for the gas stream coming out from the cyclone system using the equation (4.20);

$$\dot{V}_{G,\ in} * y_{H_2O,G,in} * \rho_{H_2O} + \dot{m}_{RM,\ in} * x_{H_2O,RM,\ in} + \dot{V}_{A,\ \ AFM\ in} * y_{H_2O,A,\ in} * \rho_{H_2O} = \dot{V}_{G,\ F\ in} * y_{H_2O,G,F,in} * \rho_{H_2O} + (\dot{m}_{CS,\ out} + \dot{m}_{Cyclone,\ out}) * x_{H_2O,RM,\ out}$$

$$37.7 * y_{H_2O,G,in} * 0.803 + 75.98 * 0.0102 + 18.1 * 0.00607 * 0.803 = 56.8 * 0.093 * 0.803 + (52.68 + 20.32) * 0$$

$$y_{H_2O,G,in} = 0.112$$

- Available heat calculation for the bypass gas stream using the equations (4.43), (4.44) and (4.45);

For reference 0 °C;

$$Q = \dot{m}_{G,\ BP} * Cp_G * (T_{G,\ BP} - 0)$$

$$Q = 27.97 * 1100 * (265.8 - 0)\ MW$$

$$Q = 8.18\ MW$$

For end temperature 130 °C;

$$Q_{LP} = \dot{m}_{G,\ BP} * Cp_G * (T_{G,\ BP} - T_{ref})$$

$$Q_{LP} = 27.97 * 1100 * (265.8 - 130)\ MW$$

$$Q_{LP} = 4.19\ MW$$

For end temperature 50 °C;

$$Q_{HW} = \dot{m}_{G,\ BP} * Cp_G * (T_{G,\ BP} - T_{ref})$$

$$Q_{HW} = 27.97 * 1100 * (130 - 50)\ MW$$

$$Q_{HW} = 2.47\ MW$$

Model validation;

- Energy balance for the gas separation point using the equation (4.21);

$$\dot{m}_{G,\ in} * Cp_G * T_{G,\ in} + P_{HGF} = \dot{m}_{G,\ BP} * Cp_G * T_{G,\ BP} + \dot{m}_{G,\ AFM\ in} * Cp_G * T_{G,\ AFM\ in} + Q_{loss}$$

$$Q_{in,\ GS} = \dot{m}_{G,\ in} * Cp_G * T_{G,\ in} + P_{HGF}$$

$$Q_{in,\ GS} = 52.3 * 1100 * 265.8 + 180 * 1000\ MW$$

$$Q_{in,\ GS} = 15.47\ MW$$

$$Q_{out,\ GS} = \dot{m}_{G,\ BP} * Cp_G * T_{G,\ BP} + \dot{m}_{G,\ AFM\ in} * Cp_G * T_{G,\ AFM\ in} + heat\ loss$$

$$Q_{out,\ GS} = 27.97 * 1100 * 265.8 + 24.3 * 1100 * 257.01 + (32000 + 18000 + 23000)\ MW$$

$$Q_{out,\ GS} = 15.12\ MW$$

- Energy balance for the AFM using the equation (4.27);

$$\dot{m}_{G,\ AFM\ in} * Cp_G * \left(T_{G,\ AFM\ in} - T_{G,\ AFM\ out}\right) + P_M = (\dot{m}_{CS,\ out} + \dot{m}_{Cyclone,\ out}) * Cp_{RM} * (T_{RM,\ out} - T_{RM,\ in}) + \dot{m}_{A,\ AFM\ in} * Cp_A * (T_{G,\ AFM\ out} - T_{A,\ in}) + \dot{m}_{RM,\ in} * x_{H_2O,\ RM,\ in} * \left[L + Cp_{H_2O} * \left(T_{G,\ AFM\ out} - T_{RM,\ in}\right)\right] + Q_{loss}$$

$$Q_{input,\ AFM} = \dot{m}_{G,\ AFM\ in} * Cp_G * \left(T_{G,\ AFM\ in} - T_{G,\ AFM\ out}\right) + P_M$$

$$Q_{input,\ AFM} = 24.3 * 1070 * (257.01 - 53.35) + 1.2 * 10^6\ MW$$

$$Q_{input,\ AFM} = 6.49\ MW$$

$$Q_{gain,\ AFM} = (\dot{m}_{CS,\ out} + \dot{m}_{Cyclone,\ out}) * Cp_{RM} * (T_{RM,\ out} - T_{RM,\ in}) + \dot{m}_{A,\ AFM\ in} * Cp_A * (T_{G,\ AFM\ out} - T_{A,\ in}) + \dot{m}_{RM,\ in} * x_{H_2O,\ RM,\ in} * \left[L + Cp_{H_2O} * \left(T_{G,\ AFM\ out} - T_{RM,\ in}\right)\right] + heat\ loss$$

$$Q_{gain,\ AFM} = (52.68 + 20.32) * 820 * (53.35 - 0) + 23.4 * 1006 * (53.35 - 5) + 75.98 * 0.0102 * [2257000 + 4184 * (53.35 - 0)] + 30000 + 103000\ MW$$

$$Q_{gain,\ AFM} = 6.39\ MW$$

- Oxygen balance for the AFM using the equation (4.15);

$$\dot{V}_{G,\ AFM\ out} * y_{O_2,\ G,\ AFM\ out} = \dot{V}_{G,\ \ AFM\ in} * y_{O_2,\ \ AFM\ in} + \dot{V}_{A,\ \ AFM\ in} * y_{O_2,\ A,\ in}$$

$$36.6 * 0.133 = 17.5 * 0.075 + 18.1 * y_{O_2,\ A,\ in}$$

$$y_{O_2,\ A,\ in} = 0.197$$

Appendix E: Possible LP steam and hot water generation calculation

- LP steam production calculation using equation (5.1);

$$Q_{LP} * 10^3 = \dot{m}_{steam} * h_s(140\ °C)$$
$$4.19 * 10^3 = \dot{m}_{steam} * 2733$$
$$\dot{m}_{steam} = 1.533\ kg/s$$

- Hot water production calculation using equation (5.2);

$$Q_{HW} * 10^6 = \dot{m}_{H_2O} * Cp_{H_2O} * \left(T_{HW,\ out} - T_{HW,\ in}\right)$$
$$2.47 * 10^6 = \dot{m}_{H_2O} * 4185 * (60 - 0)$$
$$\dot{m}_{H_2O} = 9.83\ kg/s$$

Appendix F: Detail calculation for inlet gas moisture fraction estimation for Type HS

- From equation (5.5)**;**

$$P_N * \dot{V}_{G,\ in} * y_{H_2O,\,G,\,in} = \frac{\dot{m}_{H_2O,in} * R * T_N}{M_{wH_2O}}$$

$$101325 * 37.8 = \frac{\dot{m}_{H_2O,in} * 8.314 * 273.15}{0.018}$$

$$\dot{m}_{H_2O,in} = 3.4\ kg/s$$

- From equation (5.6);

$$\dot{m}_{H_2O,CT,in} = \dot{m}_{H_2O,in} - \dot{m}_{H_2O,CT}$$

$$\dot{m}_{H_2O,CT,in} = (3.4 - 0.93)\ kg/s$$

$$\dot{m}_{H_2O,CT,in} = 2.5\ kg/s$$

- From equation (5.7);

$$P_N * \dot{V}_{CT,in} * y_{H_2O,CT,in} = \frac{\dot{m}_{H_2O,CT,in} * R * T_N}{M_{wH_2O}}$$

$$101325 * 37.1 * y_{H_2O,CT,in} = \frac{2.5 * 8.314 * 273.15}{0.018}$$

$$y_{H_2O,CT,in} = 8.3\ \%$$

Appendix G: Detail calculation for lumped capacitance method

- Residence time calculation using equation (5.16);

$$t_f = \frac{\rho_{RM} * Cp_{RM} * D_p}{6 * h} * ln\left[\frac{T_i - T_\infty}{T_f - T_\infty}\right]$$

$$t_f = \frac{1522 * 910 * 9 * 10^{-5}}{6 * 30} * ln\left[\frac{15 - 164.25}{65.5 - 164.25}\right] s$$

$$t_f = 0.286\ s$$

- Characteristic length calculation using equation (5.18);

$$L_c = \frac{V}{A_s}$$

$$L_c = \frac{\frac{4}{3} * \pi * \left(\frac{D}{2}\right)^3}{4 * \pi * \left(\frac{D}{2}\right)^2} = \frac{D}{6}$$

$$L_c = \frac{9 * 10^{-5}}{6}\ m$$

$$L_c = 1.5 * 10^{-5}\ m$$

- Biot number calculation using equation (5.18);

$$Bi = \frac{h * L_c}{k}$$

$$Bi = \frac{30 * 1.5 * 10^{-5}}{1.3}$$

$$Bi = 0.00034$$

Appendix H: Heat capacity relationships

Component	Equation number	A	B	C	D	E
N_2	1	29105	8614.9	1701.6	103.47	909.79
CO_2	1	29370	34540	-1428	26400	588
O_2	1	29103	10040	2526.5	9356	1153.8
H_2O	1	33359	26798	2609.3	8888	1167.6
SO_2	1	33375	25864	932.8	10880	423.7
Dust/limestone	2	-15500	582.3	-1.067	0.000714	0

C_p values given by equation 1 and 2 are in units $J/kmol/K$ [16].

Equation 1: $$C_p = A + B\left[\frac{\left(\frac{C}{T}\right)}{\sinh\left(\frac{C}{T}\right)}\right]^2 + D\left[\frac{\left(\frac{E}{T}\right)}{\cosh\left(\frac{E}{T}\right)}\right]^2$$

Equation 2: $$C_p = A + BT + CT^2 + DT^3 + ET^4$$